ZmDRR206 involves in maintaining cell wall integrity during maize seedling growth and interaction with the environment

Tao Zhong[1], Suining Deng[1], Yanmei Li[1], Xingming Fan[2], Mingliang Xu[1], and Jianrong Ye[1]

[1]China Agricultural University
[2]Yunnan Academy of Agricultural Sciences

August 1, 2022

Abstract

Plants adaptively change their cell wall composition and structure during growth, development, and interactions with environmental stresses. Dirigent proteins (DIRs) contribute to environmental adaptations by dynamically reorganizing the cell wall and/or by generating defense compounds. We established that maize DIR ZmDRR206 (DISEASE RESISTANCE RESPONSE206) mediates maize seedling growth and disease resistance response by coordinately regulating biosynthesis of cell wall components for cell wall integrity (CWI) maintenance. *ZmDRR206* responded to pathogen infection by rapidly increasing its expression. Both mutation and overexpression of *ZmDRR206* resulted in similar small kernel and diminished seedling growth; while *ZmDRR206*-overexpression increased disease resistance, greater drought tolerance and reduced photosynthetic activity, thus caused maize seedlings to show a growth-defense trade-off phenotype. Consistently, *ZmDRR206*-overexpression reduced the contents of primary metabolites and down-regulated the photosynthesis-related genes; while increased the contents of major cell wall components and defense phytohormones; up-regulated defense- and cell wall biosynthesis-related genes in maize seedlings grown under non-stress conditions. Furthermore, ZmDRR206 physically interacted with ZmCesA10, a secondary cell wall-specific cellulose synthase catalytic subunit, in yeast and in *planta*. Our findings unravel a mechanism that ZmDRR206 maintains CWI during maize seedling growth, providing opportunities for breeding strong disease resistance in maize.

Title

ZmDRR206 involves in maintaining cell wall integrity during maize seedling growth and interaction with the environment

Authors

Tao Zhong[1a], Suining Deng[1a], Yanmei Li, Xingming Fan[2], Mingliang Xu[1], Jianrong Ye[1*]

Affiliations

1. National Maize Improvement Center/Center for Crop Functional Genomics and Molecular Breeding, China Agricultural University, 2 West Yuanmingyuan Road, Beijing 100193, China
2. Yunnan Acad Agr Sci, Inst Food Crops, Kunming, Yunnan, Peoples R China
3.

Correspondence

* Email: yejr2006@cau.edu.cn,[a] These authors contributed equally to this work.

Summary Statement It is of critical importance for crops to correctly and efficiently allocate their resources between growth and defense to optimize fitness.*ZmDRR206* positively regulates the basal immunity for stalk

rot disease resistance by coordinately regulating biosynthesis of cell wall components for cell wall integrity (CWI) maintenance, while negatively associates with photosynthesis, thus sheds light on how maize integrates growth, the overall cell wall biosynthesis and biotic stress adaptation.

Summary

Plants adaptively change their cell wall composition and structure during growth, development, and interactions with environmental stresses. Dirigent proteins (DIRs) contribute to environmental adaptations by dynamically reorganizing the cell wall and/or by generating defense compounds. We established that maize DIR ZmDRR206 (DISEASE RESISTANCE RESPONSE206) mediates maize seedling growth and disease resistance response by coordinately regulating biosynthesis of cell wall components for cell wall integrity (CWI) maintenance. *ZmDRR206* responded to pathogen infection by rapidly increasing its expression. Both mutation and overexpression of *ZmDRR206* resulted in similar small kernel and diminished seedling growth; while*ZmDRR206*-overexpression increased disease resistance, greater drought tolerance and reduced photosynthetic activity, thus caused maize seedlings to show a growth-defense trade-off phenotype. Consistently,*ZmDRR206*-overexpression reduced the contents of primary metabolites and down-regulated the photosynthesis-related genes; while increased the contents of major cell wall components and defense phytohormones; up-regulated defense- and cell wall biosynthesis-related genes in maize seedlings grown under non-stress conditions. Furthermore, ZmDRR206 physically interacted with ZmCesA10, a secondary cell wall-specific cellulose synthase catalytic subunit, in yeast and in *planta*. Our findings unravel a mechanism that ZmDRR206 maintains CWI during maize seedling growth, providing opportunities for breeding strong disease resistance in maize.

Keywords: cell wall integrity, Dirigent protein ZmDRR206, cell wall biosynthesis, defense response, seedling growth

Introduction

The plant cell wall plays critical roles in defining cell shape and size, providing structural support for the plant body, protecting cells from invading pathogens, and acting as nodes of communication between the symplast and apoplast. Thus, cell walls are essential elements underlying growth and defense to biotic and abiotic stresses, both of which influence crop yield. Cell wall composition and structure are under active modification during various biological processes and stress responses. Maintaining cell wall integrity (CWI) is crucial for plant growth, development, and interactions with the environment; likewise, the regulatory processes controlling active and adaptive modifications of cell wall composition and structure are important for growth and defense (Engelsdorf et al., 2018; Gigli-Bisceglia et al., 2020). The*in vivo* cell wall damage (CWD) would be caused by developmental processes (cell elongation), abiotic stress factors (drought, salt, or cold), or a pathogen breaking down the cell wall during infection. If the cell experiences CWD, the cell wall becomes distorted, which is detected by CWI monitoring components and leads to growth arrest. In response, the production of lignin, jasmonic acid (JA), and salicylic acid (SA) increases to activate general stress responses. Thus, higher phytohormone (JA/SA) levels and lignin deposition are classic hallmark responses of CWI impairment. Plant cells must correct detrimental alterations to their cell wall to support growth upon a challenge to the CWI. For subsequent growth recovery, plant cells must regain their ability to loosen their walls and incorporate new polymers to avoid wall failure (Rui et al., 2020; Vaahtera et al., 2019).

The plant cell wall is a highly dynamic structure composed of several groups of polysaccharides (cellulose, hemicelluloses, pectins), structural proteins, and phenolic compounds (Lampugnani et al., 2018). Flavonoids, lignins, lignans, and monolignols are major phenolic compounds and plant secondary metabolites that are derived from the phenylpropanoid pathway and play important roles in plant biotic defense and abiotic stress tolerance. Lignin and lignan are phenolic polymers that incorporate the three monolignols coniferyl, sinapyl, and*p* -coumaryl alcohol (Ralph et al., 2019). Bimolecular phenoxy radical coupling is especially important for the biosynthesis of lignin and lignan during vascular plant development. Oxidases, like peroxidases (PODs) and laccases (LACs), are required for the formation of the monolignol radicals and have been

reported to be involved in monolignol oxidation during lignin and lignan biosynthesis (Davin and Lewis, 2000). Coniferyl alcohol (CA) is oxidized by peroxidase/H_2O_2 or LAC/O_2 to produce the corresponding radical and then dirigent proteins (DIRs) guide the phenoxy radical coupling reaction and mediate the stereoselective formation of either (+) or (-)-pinoresinol (Davin and Lewis, 2003; Pickel et al., 2010). DIRs have no catalytic activity on their own or with a suite of potential cofactors, but direct the outcome of bimolecular phenoxy radical coupling reactions toward regio- and stereospecific products in the presence of oxidases. Thus, DIRs establish their central role in plant secondary metabolism, especially the biosynthesis of lignan, flavonolignan, and alkaloids. DIRs have been identified as extracellular glycoproteins with a high β-strand content in all reported land plants. Several genes encoding (+)- or (−)-pinoresinol-forming DIRs have been described in various plant species (Dalisay et al., 2015; Gasper et al., 2016; Seneviratne et al., 2015).

It is critical to control the spatial deposition of lignin during defense responses to biotic or abiotic stress. The participation of DIRs in this process was first supported by their co-localization with lignin initiation sites, as determined by immunohistochemistry with anti-DIR polyclonal antibodies (Paniagua et al. , 2017). The casparian strip (CS) is mainly composed of lignin and constitutes a physical and chemical barrier that tightly controls water and nutrient transport and provides protection against soil-borne pathogens (Geldner, 2013). The localization of CS domain proteins (CASPs) specifies the site of CS formation in cell membrane domains by recruiting proteins required for CS formation and lignification. The DIR domain-containing protein AtDIR10/ESB1 is targeted to the lignification initiation sites in a CASP-dependent manner during CS formation in Arabidopsis and is required in both the early deposition of lignin patches and their fusion in generating the mature CS (Hosmani et al., 2013; Roppolo et al. , 2011). The soybean (*Glycine max*) DIR-like protein PDH1 is involved in regulation of soybean pod dehiscence by controlling lignin spatial deposition (Funatsuki et al., 2014). Furthermore, Arabidopsis DIR7/WSR1 plays a role in CWI maintenance, as loss of DIR7 function causes alterations in cell wall structure, impaired isoxaben (ISX, a cellulose biosynthesis inhibitor)-induced SA accumulation, and increased susceptibility to a necrotrophic fungus (Engelsdorf et al. , 2019). Thus, DIRs may exert essential functions in regulating cell wall modification/reinforcement during CWI maintenance by controlling the spatial deposition of lignin.

Lignin biosynthesis plays an essential role in plant defense responses to biotic and abiotic stresses. Lignin confers stability and hydrophobicity to the plant vascular system; lignin also forms a barrier against microbial pathogens to limit the spread of pathogen-derived toxins and enzymes into the host by altering the compressibility and porosity of the cell wall (Bacete et al., 2018; Miedes et al., 2014). The participation of DIRs in the response to pathogens that cause physical damage to the cell wall during infection has been reported in various species, whereby DIRs regulate the dynamic reorganization of the cell wall and/or generate defense compounds. The dirigent-like protein GhD2 modulates disease resistance by interacting with GhJAZ2, a member of the Jasmonate-ZIM-domain (JAZ) family, in cotton (He *et al.* , 2018). Various lignan stereoisomers display antibacterial activities. (+)-Gossypol is a phenolic aldehyde that plays an important role in pathogen responses, and DIR proteins participate in the formation of the phenolic terpenoid (+)-gossypol in cotton (*Gossypium* sp.) (Effenberger et al., 2015). *AtDIR12 /DP1* is specifically expressed in outer integument cells of developing seeds and is co-expressed with the laccase gene *LAC5* to regulate neolignan biosynthesis in Arabidopsis (Yonekura-Sakakibara et al. , 2021). In plants exposed to abiotic stress, lignification levels are frequently modulated by DIRs and peroxidases. The rise of PEROXIDASE5 and DIR2-like protein abundance in soybean coincided with elevated accumulation of H_2O_2 in roots induced by manganese (Mn) toxicity (Chen et al., 2016). These DIR-related mechanisms may support the ability of plants to cope with various abiotic stresses, a specific response to which may be provided by the mobilization of specific peroxidases and DIRs (Paniagua et al., 2017).

Maize is a major crop used for food, feed, and fuel. The more frequent occurrence of extreme weather conditions and various maize diseases often cause severe yield loss. Therefore, new maize varieties with strong disease resistance, high yield, and good quality are a constant goal for maize breeding. Several mechanisms monitor and maintain the functional integrity of plant cell walls, but knowledge of the underlying genes and molecular processes and their function in growth and defense is limited. Here, we demonstrate that the

dirigent protein DISEASE RESISTANCE RESPONSE206 (ZmDRR206) plays a role in CWI maintenance during maize seedling growth and interaction with the environment. *ZmDRR206* overexpression significantly increased disease resistance against *Fusarium graminearum* infection and drought tolerance of maize seedlings, while simultaneously compromising kernel development and seedling growth in maize and Arabidopsis. Consistently,*ZmDRR206* overexpression downregulated the expression of photosynthesis-related genes but induced that of defense-related genes, especially genes encoding enzymes for cell wall biosynthesis. We propose that ZmDRR206 involves in regulating cell wall production and remodeling to maintain CWI during maize seedling growth and defense responses.

Materials and methods

Plant materials and growth conditions

For generation of the transgenic, *ZmDRR206* overexpression maize plants, the full-length *ZmDRR206* cDNA sequence was obtained by RT-PCR and was cloned into a*pBXCUN* -derived binary vector to generate the construct *pUbiquitin* : *ZmDRR206* , in which *ZmDRR206* was driven by the maize *Ubiquitin*promoter (primers listed in Table S2). The plasmids were transformed into *Agrobacterium* strain EHA105, and then into the immature embryos of the *Zea mays L* . LH244 inbred lines (used as the control in the afterward experiments) by*Agrobacterium* mediated transformation. Six independent*ZmDRR206* overexpression maize transgenic events were generated, and their T_4 homozygous progenies were developed by continuous selfing and enough progenies were harvested for experiments and named as *DRR-OE* .

For the seedling-stage drought stress treatment, maize seedlings (*DRR-* OE and WT) were grown in controlled growth room conditions of 28/22 *C (day/night) at a light intensity of 500 μmolm^{-2} s^{-1} (16-h-light/8-h-night) and 40–50% relative humidity, under well-watered conditions by maintaining soil water content close to field capacity until drought treatment. Drought stress was imposed on the three-leaf seedlings by withdrawing water supply and keeping the plants under observation for the following 15 days, at the time, indications of severe withering symptom were visible in all of the WT seedlings (the leaves turned soft and drooping), then the seedlings were re-watered. Measurements were made at day 6 following the start of rewatering. The phenotypes of the seedlings were checked, the number of survived seedlings and the total seedling number were used to obtain the survival rate. The experiments were repeated for three times. The detection of the water loss rate of maize seedling leaves was done according to Zhang et al. (2021), the water losing rate was percentage of the weight of the lost water to the initial fresh weight of the given group. Data are means ± SD of three replicates. For Arabidopsis dehydration assay, 7-day-old seedlings grown on MS medium were transferred to soil, grown for 14 days under 8 h light/16 h dark conditions, and subjected to drought stress for an additional 10 days. and then wilted plants were re-watered for 5 days and the number of plants that survived to the stress and recovered their developmental phenotype was scored. The experiments were repeated for three times.

Subcellular localization analysis

To investigate ZmDRR206 subcellular localization, the coding sequence of *ZmDRR206* was cloned into a *pCaMV35S* :*GFP* vector to fuse in frame with the GFP-coding sequence and under the *Camv35S* promoter for constructing*pCaMV35S* :*ZmDRR206-GFP* vector. Partial cDNA of *ZmCesa10* that encoding the first four transmembrane domain (that is shared by all the four transcript variants of ZmCeas10) was obtained and fused in frame with the mCherry-coding sequence and under the *Super* promoter for constructing *pSuper* : *ZmCesA10p-mCherry* vector (primers listed in Table S2). *Agrobacterium* strain EHA105 containing the vector was cultured at 28°C overnight. *Agrobacterium* cells were harvested by centrifugation and resuspended with buffer (10mM MES, pH 5.7, 10mM MgCl2, and 200 mM acetosyringone) at OD_{600} = 0.8. Leaves of 5-week-old soil-grown *N. benthamiana* were infiltrated with*Agrobacterium* cultures, with/without combination for co-infiltration, carrying the vector *pCaMV35S* : *GFP* or*p CaMV35S* :*ZmDRR206-GFP* or *pSuper* : *ZmCesA10p-mCherry* for expressing GFP or ZmDRR206-GFP or *ZmCesA10p-mCherry* . The plants were incubated under 16h light/8h dark at 25°C in growth chambers. The GFP or mCherry fluorescence signals were detected 2-day-past-infiltration (dpi). Excitation wavelengths of GFP and mCherry were 488 nm and

561 nm, respectively. The emitted signals of GFP and mCherry were collected between 500 and 535 nm and between 580 and 620 nm, respectively. Fluorescence images were examined and taken with LSM 880 confocal laser microscope systems and images were processed using LSM microscope imaging software. The *pCaMV35S :ZmDRR206-GFP* construct was transferred into Agrobacterium tumefaciens strain GV3101 and transformed into Col plants using the floral dip method, to generate the*ZmDRR206*- overexpression transgenic Arabidopsis plants.

Measurement of leaf photosynthetic parameters

WT and *DRR-OE* seedlings at three leaves stage were used for the photosynthetic parameter measurements. The middle widest part of the latest expanded leaf of every seedling, that is the 2nd leaf of the12-day-after-germination (DAG) seedlings and the 3rd leaf of the 15-DAG seedlings, was used for SPAD value (leaf chlorophyll content) measurement, with a SPAD meter (SPAD-502 Plus, Konica Minolta, Inc. Tokyo, Japan) under a saturating actinic light (660 nm) with an intensity of 1100 μmol $m^{-2}s^{-1}$. The net photosynthetic rate (Pn) and transpiration rate (Tn) were evaluated from the latest expanded leaf (the 3rd leaf) of the 15-DAG seedlings with a Li-6400XT Portable Photosynthesis System (LI-COR, LiCor Inc., Lincoln, NE, USA), recorded at a saturating actinic light (660 nm) with an intensity of 1100 μmol $m^{-2}s^{-1}$, at the time from 09:00 to 12:00 in the morning under room temperature. All measurements were conducted on the middle part of the latest expanded, fully light-exposed leaves on each seedling following the manufacturer's instructions. Replicates were taken for each genotype.

F. graminearum **inoculation, disease severity scoring and seedling phenotypic analysis**

The fungal pathogen *F. graminearum* preparation and inoculation in the field were done according to Yang et al. (2010), and young seedling inoculation on primary roots at 5 days after germination (DAG) was done according to Ye et al. (2013), disease severity scoring was done according to Ye et al. (2018). Three replicates were set for each genotype with about 15 plants per replicate. The primary roots with typical symptoms were scored at 48 hour-after-inoculation (hai). For analysis of *ZmDRR206* expression level, the WT seedlings were inoculated with *F. graminearum* at 5-DAG, and sampled at 0 h, 6 h and 18 h. For comparing seedling root growth rate, the length of the 7-DAG young seedling primary roots cultured with paper-rolling were measured and shoot growth rate was measured with the soil-growth young seedlings at 12- or 15-DAG. The seedlings (WT and *DRR-OE*) were cultured in controlled growth room conditions of 28/22 *C (day/night) at a light intensity of 500 μmol$m^{-2}s^{-1}$(16-h-light/8-h-night) and 40–50% relative humidity. The experiments were repeated for at least three times.

Kernel phenotype and Cytological observation For the phenotypic analysis of *DRR-OE* maize mature kernels, the kernels from the middle part of each well-filled ears with uniform kernel set were used for photography and kernel trait measurement, and 100 kernels were measured for each ear. Kernel length, width, and thickness was measured using an image analysis method provided with SC-E software (Hangzhou Wanshen Detection Technology). Three replicates were collected for each genotype. For cytological observations, the central kernels of WT and *DRR-OE* at 16-day-after-pillination (DAP) were collected and were fixed in 50% (v/v) ethanol, 5% (v/v) acetic acid, and 3.7% (w/v) formaldehyde over 12 h at 4 °C, followed by dehydration and embedding in paraffin. Longitudinal sections from the middle part of kernels were cut using a Leica Ultracut (Leica, Germany) rotary microtome and stained with Periodic acid Schiff (PAS) according to Wang et al. (2011).

RNA-seq and RT-qPCR

For RNA-seq analysis, the seedlings were inoculated at 5-DAG and sampled at 18 hours after inoculation, at the same time, the non-inoculated seedlings were collected (˜ 6-DAG) and used for RNA extraction and deep sequencing in 2016. The young seedlings (from the three transgenic events) were cut into the mixing pool and then frozen in liquid nitrogen. Total RNA was extracted and the integrity and concentration of RNA samples were evaluated. RNA-seq libraries were constructed according to the protocol of the VAHTS mRNA-seq Library Prep Kit (Vazyme, Nanjing,China) and sequenced on the Illumina HiSeq 2500 platform to generate 150-bp paired-end reads. Read quality was checked and clean reads were mapped to the B73 reference genome

(RefGen_v4, AGPv4). Calculation and normalization of gene expression were based on the reads per kilobase per million mapped reads calculation (FPKM) using Cufflinks. FPKM values were calculated to identify differentially expressed genes (DEGs) ($P < 0.05$, $\log_2$fold-change > 1.0). GO enrichment analysis of the DEGs was performed using the agriGO singular enrichment analysis tool (http://bioinfo.cau.edu.cn/agriGO).

For quantitative real time reverse transcription PCR (RT-qPCR) analysis, WT seedlings was grown in the dark for 5 days and transferred to light for 1 h and 2 h to analyze light-responsive expression of *ZmDRR206* . The seedlings (WT and*DRR-OE*) were cultured in controlled growth room conditions for 6 days and used for expression analysis of specific genes. Total RNAs were extracted from the young seedling tissues with RNAiso Plus (Takara Bio), One microgram of total RNA was incubated with DNase I at 37 °C to remove the genomic DNA, and then the prepared RNA was used for first-strand cDNA synthesis using PrimeScript RT Master Mix (Takara, Dalian, China). Then qPCR assays were performed with the TB Green Premix Ex Taq kit (Takara) following the manufacturer's protocols on a 7500 Real-Time PCR system (Applied Biosystem) to detect specific genes. The used primers are listed in Table S2. Relative expression of gene was calculated using the relative quantification method with maize *GAPDH* (accession no. X07156) and*ZmTubulin1* as the endogenous control. The variation in expression was estimated using three independent biological replicates.

Analysis the contents of cell wall components

The 7-DAG seedling roots and 12-DAG maize seedlings were harvested, dried and homogenized to a fine powder using a mixer mill at 25Hz for two minutes. 100mg of powdered root or seedling tissue was sequentially used for measuring the contents of the major cell wall components according to that described by Zhang et al. (2021). The sugars in the supernatant were separated using an SP0810 column (Shodex) on a UHPLC system (Agilent-1260). The content of the detected sugars was calculated based on standard curves of glucose, xylose, mannose, galactose, arabinose, etc. Error bars indicate SD of three replicates.

Measurement of phytohormones

The endogenous SA, JA and ACC measurement assay was performed by Wuhan Greensword Creation Technology Co. Ltd., (Wuhan, China) (*http://www. greenswordcreation.com/index.html*) based on UHPLC-MS/MS analysis (Thermo Scientific Ultimate 3000 UHPLC coupled with TSQ Quantiva). To measure the endogenous concentrations of SA and JA, 500-mg samples of 6-DAG maize seedlings were harvested and extracted with acetonitrile. In brief, samples were frozen in liquid nitrogen, ground to fine powder, and extracted with 0.5 mL 80% acetonitrile at -20 °C for 12 h. After centrifugation (10,000g , 4 °C, 20 min), the supernatants were collected and evaporated under mild nitrogen stream at 35 °C, followed by re-dissolving in 100 μL acetonitrile for UHPLC-MS/MS analysis. Internal standards were added to each sample, and the phytohormones were measured using a standard curve. For the endogenous ACC contents measurement, 500-mg samples were frozen in liquid nitrogen, ground to fine powder, and extracted with 0.5 mL MeOH at -20 °C for 12 h. After centrifugation (10,000g , 4°C, 20 min), the supernatants were collected and evaporated under mild nitrogen stream at 35°C, followed by re-dissolving in 100 μL 50%MeOH for UHPLC-MS/MS analysis. Three replicates were collected for each sample and the endogenous concentration of phytohormone contents was expressed as ng g^{-1} FW.

Lignin analysis

Seedlings were grown for 5 days with a paper-rolling method and cultured in water. Then the seedlings with similar primary root length were chosen for ISX treatment. The root tips (˜3cm) of the 5-DAG seedlings were immerged into water contained 1mM ISX and cultured under normal growth condition for 10 h, indicated as ISX (+); the root tips that were immerged into water added the same amount of DMSO as that of the added ISX were used as control, ISX (-). Lignification in seedling roots ($n > 10$) was analyzed 10 h after start of treatment. Lignified regions were detected with phloroglucinol-HCl as described (Denness *et al.* , 2011).

Luciferase complementation image (LCI) assay

For LCI assay, the coding sequence of ZmDRR206 and the ORF of the four putative ZmDRR206-interacting

protein encoding genes were cloned into JW772 (C-terminal half of luciferase, cLUC) and JW771 (N-terminal half of luciferase, nLUC), respectively, using ClonExpress II One Step Cloning Kit (Vazyme Biotech). Partial cDNA of *ZmCesa10* that encoding the first four transmembrane domain and cDNA of *ZmDIN1* , *ZmRin1* was cloned into JW771 to produce CesA10p-nLUC, DIN1-nLUC, RIN1-nLUC; and cDNA of ZmDRR206 was cloned into JW772 to produce cLUC-DRR206 (primers were listed in Table S2). These constructs were transformed into *A. tumefaciens* (strain GV3101), after which, the *Agrobacterium*cells were cultured to OD600 = 0.8, pelleted, and suspended in a buffer (10 mM methylester sulfonate, 10 mM $MgCl_2$, and 150 mM acetosyringone, pH 5.7). Equal amounts of OD600-normalized*Agrobacterium* cultures for cLUC and nLUC constructs were mixed to a final concentration of OD600 = 1.0. Transient expression in *N. benthamiana* leaf tissues was achieved by *Agrobacterium*infiltration. The suspended cells containing the positive constructs were incubated at room temperature for ˜3 h and infiltrated into 5-week-old *Nicotiana benthamiana* leaves in different combinations using a needleless syringe. The infiltrated plants were placed at 28 °C for 48 h and then injected with1 mM luciferin (Beetle luciferin, Promega) at the initial injection site, and then the fluorescence signal was imaged using a Tanon-5200 imaging system. These experiments were independently repeated three times and each combination was infiltrated with multiple leaves at each time.

Yeast two-hybrid assay

The DUALmembrane pairwise interaction assay in yeast was used to investigate the interaction between ZmDRR206 and ZmCesA10, ZmDIN1, ZmRIN1 according to the DUALmembrane User Manual (www.dualsystems.com). ZmDRR206 coding sequence without the N-terminal signal peptide was subcloning into pBT3-SUC DUALmembrane bait vector using a ClonExpress II One Step Cloning Kit (Vazyme Biotech), to generate pBT3-SUC-DRR construct, in which ZmDRR206 was fused to the C-terminal half of ubiquitin (Cub) and the artificial transcription factor LexA-VP16. And the coding sequence of ZmDIN1, ZmRIN1 and partial cDNA of ZmCesA10 was subcloned into*sfi* I digested pPR3-N (the pPR3-N DUALmembrane prey vector)) to generate pPR3-N-RIN1, pPR3-N-DIN1 and pPR3-N-CesA10p constructs, that is, these preys were fused to the mutated N-terminal half of ubiquitin (NubG) with primers listed in Table S2. Plasmids pBT3-SUC-DRR was co-transformed into NMY51 yeast cell with pPR3-N-CesA10p, or pPR3-N-DIN1 or pPR3-N-RIN1 respectively. The combination of these prey constructs with pBT3-SUC empty, as well as the combination between pBT3-SUC-DRR and pPR3-N empty, was used as negative controls. Subsequently, the interaction was determined by spotting the resulting transformants onto synthetically defined (SD) /-Leu/-Trp and SD/-Ade/-His/-Leu/-Trp selection plates following the manufacturer's protocols (www.dualsystems.com). NMY51 displays a pink color in the absence of a protein-protein interaction, similar to the yeast strains carrying an *ade2* mutation; when NMY51 cells expressing an interacting protein pair will activate reporter gene to induce the cells to display a very faint pink to white color, depending on the strength of the interaction. **ZmDRR206-antibody production and immunoblot analysis.**

To develop the ZmDRR206-specific antibody, the PSAVLAADDDGTTC peptide was chemically synthesized and used as antigen to immunize New Zealand white rabbits in Hangzhou Huaan Biotechnology (http://huabio.bioon.com.cn/). For western blotting, total proteins were extracted from 6-DAG seedlings with protein extraction buffer (50 mM Tris-HCl, pH 7.5, 150 mM NaCl, 10 mM MgCl2, 0.2% NP-40, 5 mM DTT and 1×protease inhibitor cocktail). The membrane proteins were extracted from 6-DAG seedlings with Membrane Protein Extraction Kit (Sangon Biotech, C500049). 10 × SDS loading buffer was added into the protein samples, and the mixtures were incubated at 100 °C for 5 min. Proteins were resolved by SDS–PAGE and then transferred to a PVDF membrane. The membrane was then incubated with primary and secondary antibodies and visualized using ECL Plus reagent.

Statistical analysis The statistical analysis was conducted using Student's t-test between the WT and *DRR-OE* seedlings to determine statistical significance. The statistical significance was accepted at $P< 0.05$ (*), $P < 0.01$ (**) and $P< 0.001$ (***) for various growth or stress parameters. All gene expression analysis and statistical experiments were performed at least three times with independent samples. The data was expressed as the mean values ± SD of three replicates.

Results

ZmDRR206 expression responds rapidly to *Fusarium graminearum* infection and illumination in maize seedlings

We developed two near isogenic lines (NILs) carrying either the resistant *qRfg1* (Resistance to *F. graminearum*) allele (R-NIL) or the susceptible *qRfg1* allele (S-NIL) from the previously identified QTL *qRfg1* , which explained 36.3% of maize resistance to *F. graminearum* –induced stalk rot in the original mapping population (Yang et al. , 2010). Based on our published transcriptome dataset, we discovered that expression of *ZmDRR206*is significantly induced in infected R-NIL seedling roots, but not in infected S-NIL roots. We also detected a significant increase in*ZmDRR206* expression in response to *F. graminearum*infection of maize seedlings carrying the resistant allele for the other QTL *qRfg2* (Supporting Information: Figure S1a, b) (Ye et al., 2013; 2018). Moreover, the expression of *ZmDRR206* rose rapidly 6 and 18 h after inoculation with *F. graminearum* in seedlings from the inbred line LH244 (Figure 1a). These results suggested that ZmDRR206 exerts a similar function in enhancing disease resistance as its soybean ortholog (Seneviratne et al. , 2015), suggesting conservation of function.*ZmDRR206* was annotated as an inducible pathogenesis-related gene involved in defense response to biotic stimulus and encoded a DIR family protein with a predicted molecular function of isomerase activity. Based on published high-spatial-resolution transcriptome deep sequencing (RNA-seq) datasets, we observed that *ZmDRR206* is expressed in several tissues, such as the developing endosperm and young seedling shoots, roots, young leaves, and tassels (Chen et al., 2014), as well as in the basal endosperm transfer layer (BETL), the embryo surrounding region (ESR), the aleurone (AL), and the conducting zone (CZ) in developing maize kernels (Supporting Information: Figure S1c-e) (Zhan et al. , 2015).

Sequence analysis of the *ZmDRR206* promoter region (2,000 bp upstream of the start codon ATG) identified 12 light response–related*cis* -elements (LREs, including the motifs Sp1, I-box, Box-4, TCT, GT1-motif, G-box and AE), and 12 defense/stress response–related*cis* -elements, including *cis* -acting regulatory elements for MeJA, SA, and wound responsiveness, Box-w1 (pathogen-inducible*cis* -element), HSE (heat stress element), and MBS (MYB binding site). We also detected two GARE-motifs for gibberellic acid (GA) response and three elements for circadian control, two CAT-boxes for meristem-specific expression, three Skn-1-motifs and two GCN4 (General Control Nondepressible4) motifs for endosperm-specific expression (Supporting Information: Table S1). These responsive *cis* -acting elements suggested that ZmDRR206 may be a component of several signaling networks.

Consistent with the discovery of 12 LREs in *ZmDRR206* promoter, the expression of *ZmDRR206* was rapidly induced by light (Figure 1b). To investigate the subcellular localization of ZmDRR206, we transiently infiltrated *N. benthamiana* leaves with a construct overexpressing a *ZmDRR206-GFP* fusion (ZmDRR206 cloned in-frame and upstream of the green fluorescent protein [*GFP*] sequence) under the control of the cauliflower mosaic virus (CaMV) 35S promoter. We detected ZmDRR206-GFP fluorescence associated with the cell periphery, in contrast to the even distribution of the free GFP in the cytoplasm and the nucleus. We also noticed a punctate pattern for ZmDRR206-GFP fluorescence at the cell periphery (Figure 1c). We further prepared a specific polyclonal antibody against ZmDRR206: Cell fractionation and immunoblotting analysis of 6-day-old wild-type (WT, LH244 inbred line) seedlings revealed a strong ZmDRR206 signal only in the membrane pellet, but not among soluble proteins (Figure 1d). These results indicate that ZmDRR206 primarily localizes to the plasma membrane (PM).

The role of ZmDRR206 in maize kernel development and seedling growth

To investigate the biological function of ZmDRR206, we generated six independent maize transgenic events in the LH244 background harboring a construct overexpressing the full-length *ZmDRR206* coding sequence under the control of the maize *Ubiquitin* promoter. The transgenic events were self-crossed, and we harvested their T_4homozygous progeny, designated here *DRR-OE* , for phenotyping. Compared to the fully developed smooth kernels with bright yellow color in the WT ears, the mature kernels of *DRR-OE* ears were opaque (soft texture) with a light-yellow color. Mature *DRR-OE* kernels were visibly smaller in size and had a shriveled appearance at the bottom, compared to WT kernels (Figure 2a, b). The average hundred-kernel weight (HKW), and kernel length and width of*DRR-OE* kernels were all significantly smaller than those of the WT,

with a decrease in HKW of ˜55.6%, ˜46.4%, and ˜44.5% in the lines*DRR-OE3* , *DRR-OE4* , and *DRR-OE6* , respectively, compared to that of the WT. *DRR-OE* kernels exhibited a shrunken and reduced endosperm, but embryos were very similar to the WT, thus exhibiting a significantly higher embryo:endosperm ratio than the WT. Importantly, the germination rate of *DRR-OE* lines was comparable to that of the WT (Supporting Information: Figure S2a-e; Figure 2c,d). These results suggest that *ZmDRR206* overexpression impairs endosperm development but has no effect on embryo development or seed germination. The unloading of nutrients from the maternal placenta and their passage through the transfer tissue of BETL and the basal intermediate zone (BIZ) to the upper part of the endosperm influence maize kernel weight considerably. The BETL of WT kernel displayed a characteristic slightly elongated shape with labyrinth-like wall in-growths, while the BETL cells of *DRR-OE* exhibited shorter in length with fewer thickenings or wall in-growths. Compared to the extremely elongated BIZ cells with wall in-growths that decreased gradually from the second to the fourth cell layers in WT kernels, the elongation was less pronounced in *DRR-OE* kernels, and most of its cells were short, fattened or rounded like those of the starchy endosperm (Figure 2e). These results suggested that the *DRR-OE*endosperm develops dysfunctional nutrient transfer cells, especially the BETL and BIZ cells, and this may retard nutrient transport from the maternal tissue to endosperm.

Relative *ZmDRR206* transcript levels were significantly higher in the primary roots of *DRR* -OE lines, as determined by reverse-transcription quantitative PCR (RT-qPCR), with a fold increase of 175.85 in *DRR-OE3* and of 38.8 in *DRR-OE6* , compared to WT seedlings 6 days after germination (DAG). ZmDRR206 protein also accumulated to much higher levels in transgenic seedlings compared to the WT based on immunoblot analysis with the ZmDRR206-specific antibody (Figure 3a,b). Both primary root length of 7-DAG seedlings and the height of 12-DAG seedlings were shorter in the *DRR-OE3* and*DRR-OE4* lines relative to WT seedlings, but not *DRR-OE6* roots (Figure 3c-f). *DRR-OE* plants grew more slowly than the WT during the early growth stage (˜8 weeks in the field), which may partially explain the defective endosperm observed in these lines. However, *DRR-OE*plants later resumed a WT stature, and there were no obvious differences between the WT and *DRR-OE* in mature plant height. *ZmDRR206*overexpression also retarded growth of the transgenic Arabidopsis seedling, which had shorter root and silique than that of Columbia (Col) wild-type seedling (Supporting Information: Figure S2f,g). These growth dynamics (delayed early growth) suggest that ZmDRR206 may not affect the overall plant growth and development.

From EMS-induced maize mutant library (Lu et al., 2018), a mutant had a change of C-to-T at 176 bp in the only one exon of *ZmDRR206*(changes a serine to a premature stop codon), was obtained and named as*drr206* . The kernel of *drr206* was small and shrivel, with significantly smaller HKW and kernel width than that of the WT. The*drr206* seedling was smaller than that of WT, with significantly smaller primary root length. Its young leaves were green as that of the WT leaves at 8-DAG. However, the newly-expanded leaves (the 2nd leaf) of the 15-DAG seedlings were chlorotic, and the latest-grown leaf bottom of the severely chlorotic seedling was etiolated (Supporting Information: Figure S3a-e), such seedling died at ˜ 20 DAG and no homozygous progenies could be obtained. Furthermore, association analysis with data for HKW from 513 diverse maize inbred lines was downloaded from MaizeGo (*http://www.maizego.org/*), using the method of Yang *et al.* , (2014), demonstrating that*ZmDRR206* was significantly associated with HKW (Supporting Information: Figure S3f). This suggest that ZmDRR206 is important for maize seedling growth and kernel development.

ZmDRR206 influences photosynthetic activity and secondary metabolism during maize seedling growth

As the expression of *ZmDRR206* was light inducible and the growth of the *DRR-OE* seedlings was retarded, we measured chlorophyll contents and net photosynthetic rates (Pn) of *DRR-OE* seedlings and WT seedlings. We estimated chlorophyll contents by measuring the soil plant analysis development (SPAD) value at the center of the widest part of the newest expanded leaf for each seedling. As the*DRR3-OE* seedlings were much smaller than WT seedlings, we focused on *DRR-OE4* and *DRR-OE6* seedlings. The average SPAD value of 12-DAG WT leaves was 34.3, while that of 12-DAG *DRR-OE* leaves was lower by ˜22.9% (*DRR-OE4*) and ˜18.6% (*DRR-OE6*). The average SPAD values from 15-DAG *DRR-OE4* and *DRR-OE6* leaves were

also lower compared to the WT. We also measured Pn in the same leaf region of 15-DAG seedlings as for SPAD. The Pn values ranged from 11.3 to 12.7 μmol CO2 m^{-2} s^{-1} in the WT and from 6.7 to 7.5 μmol CO2 m^{-2} s^{-1} in*DRR-OE* seedlings, corresponding to a decrease of ˜44.9% (*DRR-OE4*) and ˜38.2% (*DRR-OE6*) compared to WT seedlings (Figure 3g,h). These results indicate that ZmDRR206 is negatively associated with chlorophyll biosynthesis and photosynthetic activity of seedlings, which might contribute to the delayed growth seen with *DRR-OE* seedlings.

To further explore the role of ZmDRR206 in photosynthetic activity, metabolite profiling based on high-performance liquid chromatography/mass spectrometry (HPLC/MS) was used to identify differentially abundant metabolites in the 2nd leaves of *DRR-OE* seedlings. The contents for all detected carbohydrates, organic acids, and four amino acids decreased (<0.65-fold) in the leaves of *DRR-OE* seedlings compared to the WT, while the contents of asparagine, valine, lysine, protectants (allantoin, choline, and melanin), and benzoxazinoid derivatives like DIBOA-glucoside, DIBOA, and HMBOA increased (>1.5-fold). However, the contents of different flavonoids varied, contents of flavones (vitexin, isovitexin, and luteolin), and flavanone (naringenin) rose, the contents of flavonols (kaempferol and quercetin) decreased in *DRR-OE* seedlings relative to the WT. Notably, the contents of cinnamic acid showed the biggest fold-change increase (77.6-fold) (Supporting Information: Figure S4). These results indicate that ZmDRR206 affects both primary and secondary metabolism in maize seedlings.

DRR-OE seedlings exhibit greater disease resistance and drought tolerance

Nutrient limitation typically results in competition for limited resources between growth and defense responses, such that the reallocation of energy to defense generally comes at the expense of plant growth (Huot *et al.* , 2014). As *ZmDRR206* expression was significantly induced in R-NIL plants after inoculation with*F. graminearum* , we examined the disease phenotypes of*DRR-OE* plants. We observed that *DRR-OE* seedlings exhibit higher disease resistance against *F. graminearum* infection, as evidenced by their lower disease severity index (DSI) relative to WT seedlings. Importantly, *DRR-OE* seedlings also displayed better growth of both shoots and roots after inoculated with *F. graminearum* , compared to WT seedlings. We confirmed this enhanced disease resistance against *F. graminearum* infection in field trials of mature maize plants (Figure 4). These data demonstrate that ZmDRR206 positively regulates maize disease resistance against*F. graminearum* induced stalk rot.

Unexpectedly, we discovered that *DRR-OE* seedlings are much more tolerant to drought stress; water withholding after the two-leaf stage resulted in severe wilting of all WT seedlings at ˜25-DAG, in sharp contrast to the green and upright leaves and stems of *DRR-OE*plants. We quantified this apparent tolerance to drought by scoring survival rate (SR) and leaf water lose rate (WLR) of *DRR-OE* and WT seedlings. The SR of both*DRR-OE4* and *DRR-OE6* seedlings was over 95% upon drought stress treatment, whereas WT seedlings only reached about 50% survival. Consistent with this observation, leaf WLR was lower in *DRR-OE4*and *DRR-OE6* seedlings than for WT seedlings (Figure 5a-c). We also estimated the transpiration rate (TR) at the center of the widest part of the newest expanded leaf of 15-DAG seedlings. TR values ranged from 0.88 to 0.96 μmol H_2O $m^{-2}s^{-1}$ for WT seedlings, but were much lower in*DRR-OE* seedlings, with a range from 0.50 to 0.55 μmol H_2O m^{-2} s^{-1} in*DRR-OE* seedlings or a ˜46.15% (*DRR-OE4*) and ˜40.4% (*DRR-OE6*) decrease (Figure 5d). Similarly, ZmDRR206-overexpression in Arabidopsis also increased the drought tolerance of the transgenic seedlings, which showed significantly increased SR and better growth behavior under severe water deficiency (Figure 5e, f). These results indicate that ZmDRR206 plays a positive role in drought tolerance during seedling growth.

ZmDRR206 overexpression downregulates photosynthesis- and translation-related genes

We conducted transcriptome deep sequencing (RNA-seq) to assess the effects of *ZmDRR206* overexpression on gene expression in control maize seedlings (WT and DRR) and maize seedlings inoculated with*F. graminearum* (WTi and DRRi). We identified 2,101 differentially expressed genes (DEGs) by comparing gene expression between*DRR-OE* and WT seedlings (P-value < 0.05, absolute fold change > 2.0), of which 775 were upregulated and 1,326 were downregulated (Figure 6a), thus implying that ZmDRR206 plays an

important role in maize seedling growth under normal conditions. Statistical Gene Ontology (GO) term enrichment analysis revealed the cellular components of the proteins encoded by the downregulated DEGs: ribosome (190 genes), ribonucleoprotein complex (208 genes), photosystem (34 genes), plastoglobules (20 genes), photosynthetic membrane (38 genes), macromolecular complex (278 genes), and ribosomal subunits (153 genes). The downregulated DEGs also showed an enrichment in translation- and photosynthesis-related functional categories, such as ribosome, ribosome biogenesis, ribonucleoprotein complex biogenesis, photosynthesis antenna proteins, photosynthesis light harvesting, and photosynthesis (Figures 6b,c and 7a), suggesting a reduced ability of*DRR-OE* in these processes, ZmDRR206 is negatively associated with photosynthesis and translation.

We independently validated the repression of photosynthesis by Tandem Mass Tag (TMT)–labeled quantitative proteomics of whole protein extracts from young maize leaves (2^{nd} leaf of the 12-DAG seedling). We identified 376 proteins with different abundance (DAPs) by comparing protein levels in *DRR-OE* and WT leaf extracts. 168 DAPs were predicted to localize to the chloroplast and 108 of them showing lower abundance in *DRR-OE* samples. All DAPs enriched in the Kyoto Encyclopedia for Genes and Genomes (KEGG) pathways zma00195 (photosynthesis), zma00910 (nitrogen metabolism), and zma00196 (photosynthesis-antenna proteins) exhibited a lower abundance in*DRR-OE* seedlings relative to the WT. More abundant DAPs were mainly enriched in the KEGG pathways zma00940 (phenylpropanoid biosynthesis), zma04626 (plant–pathogen interaction), zma00480 (glutathione metabolism), and zma03410 (base excision repair) (Supporting Information: Figure S5).

Among the dramatically downregulated genes in *DRR-OE* seedlings, the trihelix transcription factor gene *ZmGT-3b* exhibited an expression profile similar to that of photosynthesis-related genes (Figure 7b). ZmGT-3b interacts with ZmHY5 (maize ortholog to ELONGATED HYPOCOTYL5) to regulate maize seedling growth (Zhang *et al.* , 2021). The transcripts for*ZmGT-3b* and three randomly selected photosynthesis genes,*PHOTOSYSTEM II3* (*ZmPSII3*), *LIGHT HARVESTING COMPLEX II* (*ZmLHCII*) and *mesophyII7* (*ZmLHCII7*), was reduced to less than 0.4 in *DRR-OE4* and *DRR-OE6* seedlings compared to the WT, as seen in our RNA-seq data and by RT-qPCR (Figure 7b,c). These observations were consistent with the lower photosynthetic rates of *DRR-OE* seedlings relative to the WT (Figure 3h), suggesting that ZmDRR206 may modulate photosynthetic activity and the expression of photosynthesis-related genes during maize seedling growth. We therefore hypothesized that the retarded growth of *DRR-OE*seedlings might be associated with the repression of growth-promoting (translation- and photosynthesis-related) genes.

Defense-related transcriptional reprogramming was induced by *ZmDRR206* overexpression

Functional annotations of the DEGs upregulated by *ZmDRR206*overexpression revealed their association with oxidoreductase activity, monooxygenase activity, peroxidase activity, and ion binding (Figure 6c). KEGG pathway enrichment analysis emphasized gene functions in the biosynthesis of secondary metabolites, phenylalanine metabolism, phenylpropanoid biosynthesis, plant–pathogen interaction, and plant hormone signal transduction. Among the pathways related to biosynthesis of secondary metabolites, biosynthesis of flavone, flavonol, stilbenoid, diarylheptanoid, gingerol, benzoxazinoid, diterpenoid, flavonoid, and isoflavonoid was significantly enriched (Figure 6b). This result was consistent with the above metabolome analysis, which showed various changes in benzoxazinoids and flavonoids (Supporting Information: Figure S4). Almost all of these functional categories can be summarized in support of basal defense responses to various biotic/abiotic stresses, suggesting that ZmDRR206 is positively associated with plant defense responses.

Upon induction of plant immune responses, plants undergo a substantial transcriptional reprogramming to prioritize defense- over growth-related cellular functions. Inoculation with *F. graminearum* induced 1,026 DEGs in WT seedlings, including 304 DEGs that were also induced by*ZmDRR206* overexpression, pointing to commonalities in the transcriptional reprogramming induced by *ZmDRR206* overexpression (DRR/WT) and inoculation (WTi/WT). DEGs induced by inoculation (WTi/WT) were also significantly enriched for GO and KEGG terms related to biosynthesis of secondary metabolites, especially biosynthesis of phenylpropanoid, stilbenoid, diarylheptanoid, gingerol, benzoxazinoid, flavonoid, diterpenoid, flavone, flavonol, carotenoid, and

phenylalanine metabolism. Notably, the transcriptional reprogramming induced by *ZmDRR206* overexpression (DRR/WT) was stronger for these defense response–related functional categories than that induced by inoculation of WT seedlings (WTi/WT), as indicated by their greater number of DEGs in DRR/WT relative to the WTi/WT comparison (Supporting Information: Figure S6). Therefore, *ZmDRR206* overexpression induced defense-related transcriptional reprogramming in *DRR-OE* seedlings.

Furthermore, 708 genes were differentially expressed in inoculated *DRR-OE* seedlings compared to inoculated WT seedlings (DRRi/WTi), of which 180 DEGs were also identified as DEGs in the non-inoculated DRR/WT comparison. The top-enriched defense-related KEGG pathways comprised more DEGs from the DRR/WT comparison than from the comparison between inoculated genotypes (DRRi/WTi). Compared to their respective non-inoculated seedlings, inoculation caused the differential expression of 1,026 (WTi/WT) and 2,259 (DRRi/DRR) genes in the WT and *DRR-OE* , respectively, with 400 genes differentially expressed in both genotypes (Supporting Information: Figure S7a-c), suggesting that overlapping signaling pathways may control gene expression in these two genotypes in response to inoculation. The magnitude of transcriptional reprogramming appeared to be greater upon inoculation in *DRR-OE* seedlings (DRRi/DRR) than in WT seedlings (WTi/WT), as more DEGs were enriched in all top-enriched defense-related KEGG functional categories (Supporting Information: Figure S7d). These results are consistent with the higher resistance against infection and the lower DSI observed with inoculated *DRR-OE* relative to inoculated WT seedlings (Figure 4).

Cell wall metabolism is modified and the related genes are up-regulated in *DRR-OE* seedlings

Lignin is one of the most important secondary metabolites and its defense-induced biosynthesis plays a major role in basal immunity. We thus investigated the cell wall composition of roots from 7-DAG seedlings and from 12-DAG whole seedlings. We detected a significant increase in content of acid-soluble lignin (ASL, ˜13.0%), acid-insoluble lignin (AIL, ˜11.1%), and lignin (˜11.5%) in roots of 7-DAG *DRR-OE* seedlings, while the contents for cellulose and semi-cellulose were similar, compared with WT seedlings (Figure 8a). By 12-DAG, *DRR-OE* seedlings also showed greater contents for cellulose (˜8.0%) and semi-cellulose (˜9.7%), together with increased contents for AIL (˜6.7%) and lignin (˜6.1%), although ASL contents were not different compared to WT seedlings. Arabinose levels are positively correlated with lignin levels, cellobiose can activate plant immune responses, and shifts in the xylose content of the cell wall have a deep impact on CWI and susceptibility to pathogens (Li *et al.* , 2015; Bacete *et al.* , 2018). Notably, we measured higher levels of cellobiose (˜14.1%), glucose (˜4.5%), arabinose (˜6.5%), and xylose (˜4.6%) in 12-DAG *DRR-OE* seedlings compared to WT seedlings (Supporting Information: Figure S8a, b). Furthermore, we noticed that the leaf blade and midrib are significantly thinner in 12-DAG *DRR-OE* relative to WT seedlings (Supporting Information: Figure S8c), which was consistent with the reduced photosynthetic activity of *DRR-OE* seedlings. The observed changes in contents for the main cell wall components in *DRR-OE* seedlings may increase the structural integrity and strength of the cell wall, suggesting that ZmDRR206 coordinately regulates the biosynthesis of cell wall components.

CWI signaling regulates the expression of cell wall–related genes. The influence of *ZmDRR206* overexpression on cell wall composition prompted us to assess the expression profiles of these genes in *DRR-OE* seedlings. GO analysis revealed that many DEGs were significantly enriched in cell wall organization/biogenesis–related functional categories, including xyloglucan metabolism, hemicellulose metabolism, cell wall polysaccharide metabolism, cell wall modification, and glucan metabolism (Figure 8b), indicating these genes contribute to biosynthesis/modification of cell wall-related components, including xyloglucan, hemicellulose and glucan. Consistent with the higher contents for the major cell wall components obtained above, transcript levels for 17 *cellulose synthase* (*Ces*) genes were elevated in *DRR-OE* seedlings, compared to WT seedlings (Supporting Information: Figure S9a). Furthermore, many genes encoding the critical enzymes in the lignin biosynthesis pathway were upregulated in *DRR-OE* seedlings, including genes encoding phenylalanine ammonia-lyase (PAL), 4-coumarate CoA ligases (4CLs), caffeoyl-CoA *O* -methyltransferases (AOMTs), cinnamyl alcohol dehydrogenases (CADs), laccases (LACs), dirigent proteins (DPs) and CASP (Fig. 9Sb-d). Of the genes involved in xyloglucan metabolism and cell wall remodeling/function, including those encoding

xyloglucan galactosyltransferase, xyloglucan glycosyltransferase, xyloglucan 6-xylosyltransferase, xyloglucan endotransglucosylase/hydrolases (XTHs) and expansins (EXPs) were down-regulated; while POD, chitinase, UDP-glucosyltransferase (UGT) and ABC transporter encoding genes were upregulated in *DRR-OE*seedlings relative to WT seedlings (Supporting Information: Figure S10).

Among the upregulated cell wall biosynthesis–related genes,*ZmCesA10* , *ZmCesA11* , and *ZmCesA12* encoding cellulose synthases required for cellulose biosynthesis in secondary cell walls (Hernandez-Blanco *et al.* , 2007; Miedes *et al.* , 2014). Consistent with the increased contents of cell wall components, the transcript levels of*ZmCesA10* , *ZmCesA11* , and *ZmCesA12* , as well as those of genes encoding critical enzymes in the lignin biosynthesis pathway (*C4M* , *AOMT* ,*CAD-bm1* [also named *brown midrib*], and *CAD6*), were all significantly upregulated in *DRR-OE* seedlings relative to WT seedlings, as determined by RT-qPCR (Figure 8c). Furthermore, ISX induced ectopic production of lignin in the upper part of WT primary root tips, but not in *DRR-OE* seedling roots, as revealed by staining with phloroglucinol-HCl (an indicator of secondary wall thickening) (Figure 8d). These results indicate that ZmDRR206 plays a role in CWI maintenance by regulating cell wall production and remodeling during maize seedling growth.

The CWI maintenance system involves receptor-like kinases (RLKs) and ion channels that constantly monitor the state of the cell wall and initiate adaptive changes in both cellular and cell wall metabolisms (Engelsdorf*et al.* , 2018; Vaahtera *et al.* , 2019). Many upregulated DEGs encoded transporters or proteins with functions linked to ion binding in *DRR-OE* seedlings. In particular, multiple ion transporters were upregulated in *DRR-OE* seedlings relative to WT seedlings, including genes encoding phosphate, potassium, copper, vacuolar iron, and zinc transporters, as well as three ammonium transporter genes (Supporting Information: Figure S11a). We thus measured the mineral elemental composition of 7-DAG seedlings. Compared to WT seedlings, *DRR-OE* seedlings accumulated more magnesium (Mg), potassium (K), sodium (Na), and phosphorus (P) but presented a lower abundance of aluminum (Al) and iron (Fe). The contents for copper (Cu) and zinc (Zn) were comparable across seedlings (Supporting Information: Figure S11b), indicating that cellular osmotic conditions (ion contents) are altered in *DRR-OE* seedlings. These results further suggest that ZmDRR206 may play a role in CWI maintenance.

The altered biosynthesis and signaling of the defense-related phytohormones and the constitutive expression of defense-related genes in *DRR-OE* seedlings

The impairment of CWI imposed by ISX treatment or mutation in*CesA* triggers responses that include the activation of defense gene transcription; JA, SA, and/or ethylene production; and lignin accumulation (Cano-Delgado *et al.* , 2003; Denness *et al.* , 2011). The altered cell wall composition observed in *DRR-OE*seedlings prompted us to check the transcript levels of JA/SA and ethylene biosynthesis genes in*DRR-OE* seedlings. For JA biosynthesis, eight *lipoxygenase* (*LOX*) genes were upregulated in *DRR-OE* seedlings relative to WT seedlings, while the genes encoding allene oxide synthase (AOS) and allene oxide cyclase (AOC) did not reach statistical significance. Four *PAL* genes were up-regulated in *DRR-OE* seedlings, together with the significantly higher cinnamic acid content of the *DRR-OE* line (Figure 9a, b), indicating that both JA and SA biosynthesis are induced. Consistently, the contents of JA, JA-Ile (the bioactive form of JA), 2-oxo-phytodienoic acid (OPDA, the precursor for JA biosynthesis), and SA were all significantly increased, while ACC (the precursor for ethylene biosynthesis) content was significantly decreased in*DRR-OE* relative to that in WT seedlings (Figure 9c). In addition, JA/SA-regulated and/or defense-related genes appeared to be constitutively up-regulated in *DRR-OE* seedlings, including jasmonate-regulated genes (*JRG* s), jasmonate-induced protein genes (*JIP* s), vegetative storage protein genes (*VSP* s),pathogenesis-related genes (*PR* s), disease resistance genes (*DRP* , *RPM1* , *RPP13* , and *RPS2*), and chitinase genes (Supporting Information: Figure S12a). We confirmed the up-regulated expression of several defense-related genes in*DRR-OE* and WT seedlings by RT-qPCR, including two WRKY transcription factor genes (*WRKY11* and *WRKY69*), four*PR* genes (*PR1* , *PR10a* , *PR10b* , and*PR3*), three chitinase genes (*CHN5* [*chitinasechem5*], *AEC* [*Acidic endochitinase*], and*BEC* [*Basic endochitinase A*]), and five JA-regulated genes (two *JIP* s, *VSPpni288* , *VSP2* , and *LOX2*) (Figure 9d). Furthermore, *ZmDRR206* overexpression significantly upregulated genes belonging to multiple transcription factor (TF) families such as MYB (eight genes), WRKY (nine genes),

basic helix-loop-helix (bHLH, eight genes), ERF (13 genes), basic leucine zipper (bZIP, five genes), and NAC (seven genes). Other genes encoding growth-promoting TFs were downregulated in *DRR-OE* relative to WT seedlings, including *GATA* genes, *TCP* genes, *PRE3*genes (Supporting Information: Figure S12b). These altered patterns of gene expression further suggest that ZmDRR206 plays a role in CWI maintenance and contributes to the altered growth and stress response of*DRR-OE* seedlings.

ZmDRR206 is involved in cell wall biosynthesis through its interaction with ZmCesA10 To further investigate the molecular mechanism of ZmDRR206, we searched for interaction partners. The STRING database (https://string-db.org/cgi) suggested several candidates that we compared to our quantitative proteomics dataset (Supporting Information: Figure S5f). We also checked the expression profiles of these candidate genes in qTeller () and in our RNA-seq data, culminating in the selection of three candidates: ZmCesA10, ZmDIN1 (DARK-INDUCED1, a thiosulfate sulfur transferase), and ZmRin1 (Ribonuclease 1). We assessed their interaction potential with ZmDRR206 in a split-ubiquitin membrane-based yeast two-hybrid system (DUALmembrane system) and by luciferase complementation imaging (LCI) assay. ZmDRR206 was fused to the C-terminal half of ubiquitin (Cub), and partial *ZmCesA10* ,*ZmDIN1* , or *ZmRIN1* was fused to the mutated N-terminal half of ubiquitin (NubG). As the negative controls, the co-transformation of DRR206-Cub with the NubG empty vector didnot enable the yeast cells to grow on the selective medium. In contrast, the yeast cells co-transformed with*DRR206-Cub* and *NubG-CesA10p* ; *DRR206-Cub* and*NubG-DIN1* ; or *DRR206-Cub* and *NubG-RIN1* constructs, were able to grow on the selective medium, indicating that DRR206 and CesA10, DRR206 and DIN1, DRR206 and RIN1 interacted in yeast to activate the expression of the reporter gene for growth selection (Figure10a). In the LCI assay, we cloned the coding sequences of the potential interactors in-frame and upstream of the sequence of the N-terminal half of firefly luciferase (nLUC, in the JW771 vector) to produce*CesA10p-nLUC* , *DIN1-nLUC* , and *RIN1-nLUC* . We also cloned the coding sequence of *ZmDRR206* into JW772 (harboring the sequence for the C-terminal half of luciferase, *cLUC*) to produce*cLUC-DRR206* . We detected strong luminescence signals when the pairs of constructs *cLUC-DRR206*and *CesA10p-nLUC* ;*cLUC-DRR206* and *DIN1-nLUC* ; or *cLUC-DRR206* and*RIN1-nLUC* were co-infiltrated into *Nicotiana benthamiana*leaves, but not their negative control construct combination (Figure 10b), indicating the interaction between DRR206 and CesA10, DRR206 and DIN1, DRR206 and RIN1 *in planta* . Moreover, in contrast to the random distribution of the free GFP or mCherry in the cytoplasm and the nucleus, DRR206-GFP signal associated with the cell periphery and CesA10p-mCherry signal alone accumulated into big spots in the cell periphery (suggesting its association with specific subdomain of the PM), while DRR206-GFP signal could co-localize with CesA10p-mCherry signal in the cell periphery of the epidermal cells of *N. benthamiana* leaves and DRR206-GFP could disrupt the accumulated big spot induced by CesA10p-mCherry alone (Figure 10c).

Furthermore, we observed a marked co-expression between *ZmDRR206*and *ZmCesA10* during maize growth and development. Indeed,*ZmDRR206* and*ZmCesA10* were abundantly expressed in young shoots, roots, and leaves (leaf1 and leaf2) (Chen *et al.* , 2014). The expression of both genes was induced by *F. graminearum* inoculation after 6 h in 5-DAG roots of the resistant NIL, but not in the susceptible NIL (Ye*et al.* , 2013). Moreover, *ZmDRR206* and *ZmCesA10* were specially expressed to comparable levels in crown root nodes, non-pollinated internodes at 24 DAP, V9 eleventh leaves, V9 immature leaves, V9 thirteenth leaves, 5-day-old primary roots, 5-day-old root cortex, and 7- to 8-day-old secondary roots, based on a survey of RNA-seq data through qTeller (Supporting Information: Figure S13). These results further suggest that ZmDRR206 interacts with ZmCesA10*in vivo* to maintain CWI during maize growth and defense response.

Discussion

The plant cell wall is a complex, dynamic molecular network whose composition and structure are under constant change during development and in response to stress. Plant cells monitor the status of their cell walls with various types of sensors and receptors at the plasma membrane, some of which may interact with cell wall components to coordinate mechanical changes in cell wall structure and cellular responses (Vaahtera *et al.* , 2019). The disruption of CWI results in a variety of compensatory reactions, including ectopic deposition of lignin (Cano-Delgado *et al.* , 2003), alteration of other cell wall components (Pogorelko

et al. , 2013), ROS production (Denness*et al.* , 2011), and an increase in JA and ethylene production (Ellis *et al.* , 2002). The observed stunted growth of many cell wall mutants associated with attenuated cell wall biosynthesis may partially reflect responses mediated by constitutive activation of defense pathways and the ensuing trade-off between growth and defense, rather than being directly caused by a physically weakened cell wall (Bacete *et al.* , 2018; Bischoff *et al.* , 2009; Tsang*et al.* , 2011). Cell wall strengthening can be activated by loss of CWI via the mechanisms that monitor cell wall status. DIRs have been suggested to represent one set of potent effectors acting downstream of the CWI signaling cascade by mediating the spatial control of lignin deposition during growth and stress responses (Denness *et al.* , 2011; Paniagua *et al.* , 2017).

In this study, we demonstrated that ZmDRR206 actuates CWI maintenance and confers disease resistance in maize. We screened DEGs in two maize NILs differing at the QTL*Rfg1* after fungus infection and identified *ZmDRR206* as being strongly expressed specifically in the NIL that exhibits strong resistance against stalk rot disease resistance. There are three major findings in this study. First, we identified ZmDRR206 as a regulator of maize seedling growth and basal immunity: The abundance of this protein was positively correlated with maize disease resistance by regulating cell wall biosynthesis and defense responses, while negatively regulating photosynthesis, thus shedding light on how maize integrates growth, overall cell wall biosynthesis, and adaptation to biotic stress. Second, we showed that ZmDRR206 plays a role in CWI maintenance by coordinately regulating the biosynthesis of cell wall components. It is well known that defense-induced lignin plays a major role in basal immunity to promote plant fitness. However, gene(s) that coordinately regulates biosynthesis of cell wall components remains obscure.*ZmDRR206* overexpression increased the contents of major cell wall components and conferred resistance to ISX treatment. An interaction between ZmDRR206 and ZmCesA10 was also established. Third, we determined that the negative effect of *ZmDRR206* overexpression on physiological processes like photosynthesis and translation during maize seedling growth and defense responses, this might associate with the interaction between ZmDRR206 and different protein partners. More work is needed to understand the roles of the interactions between ZmDRR206 and ZmDIN1/ZmRIN1.

ZmDRR206 is involved in CWI maintenance during maize seedling growth and defense responses

Plant cell wall modifications through mutation or overexpression of cell wall–related genes substantially influence disease resistance and/or tolerance to abiotic stresses (Bellincampi *et al.* , 2014; Kesten*et al.* , 2017). The observed disease resistance phenotypes in the mutants/transgenic plants with wall alterations are thought to be caused by the activation of defense signaling pathways, rather than as an inability of pathogens to overcome these modified wall composition/structures (Houston *et al.* , 2016; Miedes *et al.* , 2014). Cellulose affects many aspects of plant life and fitness through its central role in determining the mechanical properties of plant cell walls. In agreement with this notion, impairing the function of CesA enzymes induces the reorganization of primary and secondary cell walls and altered wall compositions with lower cellulose biosynthesis, which causes CWD and subsequent CWI alterations that activate immune responses, like the ectopic biosynthesis and deposition of lignin, the biosynthesis of antimicrobial compounds, and the constitutively activated defense responses with increased production of JA, ethylene and ROS. However, while this global response increases disease resistance, it will also diminish plant growth, thus explaining the poor growth seen in these mutants (dwarf plants and reduced seed yield) (Cano-Delgado *et al.* , 2003; Ellis *et al.* , 2002; Escudero *et al.* , 2017; Hernandez-Blanco *et al.* , 2007; Taylor-Teeples *et al.* , 2015).

A functional cellulose synthase complex (CSC) requires the cooperation of at least three distinct CesA proteins encoded by different*CesA* genes for the biosynthesis of both primary and secondary cell walls (Cho *et al.* , 2017; Schneider *et al.* , 2017). Arabidopsis CesA8, CesA7, and CesA4 are the secondary cell wall–specific cellulose synthase catalytic subunits; their respective mutants, *irregular xylem1* (*irx1*), *irx3* , and*irx5* , display collapsed xylem and altered secondary cell wall integrity and enhanced disease resistance against multiple pathogens that are associated with altered expression of genes related to CWI (Escudero *et al.* , 2017; Hernandez-Blanco *et al.* , 2007). The constitutive activation of immune responses in *irx1/3/5*plants

probably explains their trade-off phenotypes (dwarf plants and reduced seed yield) and disease resistance phenotype. Likewise, rice (*Oryza sativa*) OsCesA7, OsCesA9, and OsCesA4 are the functional orthologs of the Arabidopsis enzymes (Tanaka *et al.,* 2003). All mutants identified in *OsCesA4* , *OsCesA7* , and *OsCesA9*share a brittle culm (bc) phenotype and abnormal plant growth, characterized by a dwarf stature with small leaves and withered leaf tips. These rice *CesA* mutants have lower cellulose contents in their secondary wall and accumulate JA and ethylene, resulting in a dwarf phenotype (Kotake *et al.* , 2011; Li *et al.* , 2017; Wang *et al.* , 2016). *DRR-OE* seedlings also displayed diminished growth; enhanced disease resistance; the concomitant rise of cellulose, semi-cellulose, and lignin contents; and increased JA and SA levels, compared to WT seedlings (Figures 3-9). Consistently, 17*CesA* genes and a subset of secondary metabolite biosynthesis-related genes, especially genes encoding enzymes for lignin biosynthesis, were constitutively upregulated, while cell wall modification-related genes like *EXP* s and *XTH* s were downregulated, in *DRR-OE* seedlings (Supporting Information: Figure S9,10). ZmCesA10 is an ortholog of OsCesA7. *ZmCesA10* ,*ZmCesA11* , and *ZmCesA12* were significantly upregulated in*DRR-OE* seedlings relative to WT seedlings (Figure 8c). We established that ZmDRR206 physically interacts with ZmCesA10 in yeast and *in planta* and that their encoding genes are co-expressed in various tissues at various developmental stages in maize (Figure 10; Supporting Information: Figure S13). ISX is a frequently used tool to impose cell wall stress in plant CWI maintenance research; notably,*DRR-OE* seedlings were resistant to ISX treatment (Figure 8d). Together with the altered cell wall composition and the cellular osmotic conditions (ion contents), the upregulation of cell wall biosynthesis-related genes, and the growth-defense trade-off phenotype of *DRR-OE* seedlings, the interaction between ZmDRR206 and ZmCesA10, we propose that ZmDRR206 coordinately regulates the biosynthesis of cell wall components and plays a role in CWI maintenance during maize seedling growth and defense responses. The similar defects in maize kernel development and seedling growth caused by*ZmDRR206* overexpression (Figures 2,3) or mutation (Supporting Information: Figure S3) suggest that the accurate regulation of CWI is critically important for these development processes, and further confirmed the role of ZmDRR206 in CWI maintenance.

Constitutive defense responses are activated by *ZmDRR206*overexpression in maize seedling

The biosynthesis of cell wall components is coordinately regulated, the metabolism and deposition of cellulose and lignin in cell walls are vital for growth and defense responses (Liu *et al.* , 2018; Ohtani and Demura, 2019). Lignin contributes to pathogen resistance, while pathogens can target the host proteasome to modify the cell wall secondary metabolism to facilitate their invasion. CAD is the final enzyme in the monolignol biosynthetic pathway and thus directly affects lignin accumulation. ZmCAD is associated with the accumulation of lignin and restricts the expansion of lesions when maize plants are infected by*Rhizoctonia solani* , the causal agent of banded leaf and sheath blight (BLSB). However, the pathogen can target ZmCAD for ubiquitination and degradation by interacting with the F-box protein ZmFBL, resulting in susceptibility to BLSB (Li *et al.* , 2019). Consistently,*ZmDRR206* over-expressing lines had enhanced cell wall biosynthesis; increased JA, JA-Ile and SA levels; and constitutive expression of many defense-related genes, including multiple *PR* s and disease resistance genes. However, it was unexpected to find the lower ACC level in *DRR-OE* seedlings, as the ethylene synthesis genes (*ACC synthase* and *ACC oxidase*), were up-regulated in*DRR-OE* relative to WT seedlings. It is possible that ACO activity might be higher than ACC activity, thus leading to more ethylene production and stronger signaling (the up-regulated *ERF* s) in*DRR-OE* relative to WT seedlings (Figure 9; Supporting Information: Figure S12). Chitinases are classic PR proteins involved in non-host-specific defense and are thought to be involved in cell wall modification and activation of ethylene production (Jiao *et al.* , 2019). XTHs are cell wall–remodeling enzymes, while EXPs are apoplastic proteins that are usually involved in cell growth or cell wall remodeling by weakening the binding between cell wall components and rendering the wall more susceptible to pathogen (Paniagua *et al.* , 2017). Plant UGTs glycosylate various phytohormones and metabolites in response to biotic and abiotic stresses, thus highlighting their unique modulations against environmental stimuli (Rehman *et al.* , 2018). Plant ABC transporters are specialized plant membrane transporters involved in import/export of various metabolites inside the cell and in regulating growth, development, tolerance to biotic and abiotic stresses, cell detoxification, and transport of phytohormones (Do *et al.* , 2018). Consistently, most of the *XTH* and *EXP* genes among

the DEGs between *DRR-OE* seedlings and the WT were downregulated, while DEGs encoding chitinase, UGT and ABC transporters were upregulated (Supporting Information: Figure S10). Melatonin plays an important role in ameliorating various common abiotic and biotic stresses, including cold, drought, heavy metals, salt and pathogen attack (Arnao & Hernández-Ruiz, 2019). The contents of the three protectants, allantoin, choline, and melanin, were all increased >1.5-fold in*DRR-OE* relative to WT seedlings (Supporting Information: Figure S4). Collectively, *ZmDRR206* overexpression activated a constitutive defense response, visible as the slow growth phenotype of*DRR-OE* seedlings from the growth–defense trade-off.

ZmDRR206 may affect different physiological pathways by physically interacting with various proteins. Indeed, we determined that ZmDRR206 interacts with ZmDIN1, which is a senescence-associated dark-inducible protein. *DIN* genes constitute the basal immune responses used by cells to cope with stresses imposed by senescence or pathogen infections and by SA, MeJA, darkness, or photosynthesis inhibitors (Fujiki *et al* ., 2001). A common theme to these stress conditions is cellular damage caused by oxidative stress, suggesting there may be overlapping factors interacting with ZmDRR206 that may participate in various stress-responsive pathways. Arabidopsis *DIN6* and *DIN11* are key regulators during systemic virus infection (Fernández *et al.* , 2016). The DIN1 ortholog *NbNRIP1* (*N receptor-interacting protein 1*) from *N. benthamiana* is required for an effective defense response against *Tobacco mosaic virus* (TMV) (Caplan*et al* ., 2008). Tobacco (*Nicotiana tabacum*) *Ntdin* is involved in sulfur and nitrogen metabolism due to its relationship with nitrate reductase activity and molybdenum cofactor (Moco) biosynthesis.*Ntdin* expression is also upregulated by both ABA and IAA, likely because the biosynthesis of these phytohormones requires Moco (Yang*et al.* , 2003). The physical interaction between ZmDRR206 and ZmDIN1 may thus modulate various aspects of the constitutive defense response in *DRR-OE* seedlings.

The possible role of ZmDRR206 in photosynthesis and translation

Photosynthesis affects the cellular ability to initiate a defense response by generating ROS and immune response-related signals such as SA. Pathogen infection represses photosynthesis, affects primary metabolism, slows down plant growth, and modifies secondary metabolism toward defense responses. The products of photosynthesis (sugars) can activate defense-related responses and modulate key signaling elements of defense phytohormone pathways in an attempt to strike a precise balance between growth and defense responses (Lu and Yao, 2018). An effect on photosynthetic properties by cell wall dynamics has been reported. Indeed, diffusion of CO_2 from the leaf intercellular air space to the site of carboxylation is a potential trait for increasing photosynthetic efficiency and crop productivity. Cell wall characteristics like thickness and porosity have been reported to be key traits determining mesophyll conductance (g_m) and photosynthesis, as dynamic changes in cell wall composition and rearrangements of cell wall components have been shown to affect g_m under nonstress conditions (Carriquí *et al.* , 2019, 2020; Onoda *et al.,* 2017; Veromann-Jürgenson *et al.,*2017). Modulation of photosynthesis by cell wall modifications has been demonstrated in rice mutants. For instance, knockout mutants in*Cellulose synthase-like family 6* (*OsCSLF6*) are disrupted in cell wall mixed-linkage glucan (MLG) production and have lower g_m compared to the WT, suggesting that a change in cell wall properties influences the diffusivity and availability of CO_2 (Ellsworth *et al.* , 2018). The rice*fragile culm 24* (*Osfc24*) mutant is dwarf and brittle, whose cell wall composition is altered, with lower contents of cellulose and pectin, but higher levels of hemicellulose and lignin. The*Osfc24* mutant has pale leaves with lower chlorophyll contents, as well as diminished photosynthetic activity (Zhang *et al.* , 2020). Changes in pectin physicochemical properties induce modifications in wall architecture by rearranging cell wall compounds. The Arabidopsis mutants *atpme17.2* (*pectin methylesterase17.2*) and*atpae11.1* (*pectin acetylesterase11.1*) are characterized by distinct contents of cell wall non-cellulosic neutral sugars, a lower proportion of cell wall pectin, and decreased g_m and photosynthesis (Roig-Oliver *et al.* , 2021). Collectively, these observations suggest that cell wall modifications play a substantial role in determining photosynthetic output. *ZmDRR206*overexpression repressed the expression of photosynthetic genes and activated that for cell wall formation genes. Consistently, the contents of cell wall components were higher, while chlorophyll contents and photosynthesis activity were lower in *DRR-OE* seedlings relative to the WT (Figures 3,8), and the chlorotic or etiolated leaves observed in the ZmDRR206 mutant, suggesting that ZmDRR206 affects chlorophyll biosynthesis and photosynthesis by regulating cell wall biosynthesis.

ZmRIN1 is annotated as a ribonuclease with endoribonuclease and RNA binding activity, is secreted into the extracellular region, is involved in RNA catabolism, and plays pivotal roles in RNA maturation and decay, including ribosome RNA processing and post-translational control (Court*et al.* , 2013). The physical association between ZmDRR206 with ZmRIN1 may explain the downregulation of DEGs enriched in ribosome- and translation-related functional categories in *DRR-OE* seedlings compared to the WT, reflecting a negative association between*ZmDRR206* and translation (Figure 6b,c). Ribonucleases have been proposed to provide cells with the means to recognize and destroy unwanted genetic material (Aguado and tenOever, 2018). Small RNA–mediated sequence-specific cleavage is utilized in both prokaryotes and eukaryotes to combat virus infection via the double-stranded RNA binding domain of ribonucleases. Moreover, ribonucleases are also an essential component for the generation of microRNAs (miRNAs), which are small noncoding RNAs that fine-tune protein abundance via translational repression in both the plant and animal kingdoms. miRNAs also act as a sequence-specific guides for the RNA-induced silencing complex (RISC) by binding to their cognate mRNA targets and inducing their cleavage (Court*et al.* , 2013). ZmDRR206 may thus be involved in the suppression of ribosome and translation activity through its interaction with ZmRIN1.

Together, our results indicate that ZmDRR206 likely acts as a conserved component in maize seedling growth and defense responses to external biotic/abiotic stresses through its physical interactions with different protein partners that participate in various biological processes. ZmDRR206 may positively regulate cell wall biosynthesis and modifications for CWI maintenance and immune response by physically interacting with ZmCesA10 and ZmDIN1, thus optimizing the temporal and spatial expression of growth promotion (photosynthesis and translation), cell wall biosynthesis, and defense-related genes to coordinate metabolism during seedling growth and defense response to external environmental stress. More work is needed to understand the roles of the interaction between ZmDRR206 and these proteins in plant growth and defense responses.

Acknowledgements

This work was supported by the Ministry of Agriculture and Rural Affairs of the People's Republic of China (Grant No. 2018ZX0800917B) and grant from Yunnan Provincial Science and Technology Department (202005AF150026).

Conflict of interest The authors declare that they have no conflict of interest.**Author contributions**J. Ye, T. Zhong, and S. Deng performed the research; Y. Li and X. Fan managed maize growth and inoculation in the field. M. Xu supervised this project; J. Ye designed the research, analyzed the data, wrote and revised the manuscript.

References

Aguado, L.C., tenOever, B.R. (2018) RNase III Nucleases and the Evolution of Antiviral Systems. *Bioessays,* 40(2).

Arno, M. B., Hernández-Ruiz, J. (2019) Melatonin. A new plant hormone and/or a plant master regulator? *Trends in Plant Science,* 24, 38–48.

Bacete, L., Mélida, H., Miedes, E., Molina, A. (2018) Plant cell wall-mediated immunity: cell wall changes trigger disease resistance responses. *The Plant Journal,* 93(4), 614-636.

Bellincampi, D., Cervone, F., Lionetti, V. (2014) Plant cell wall dynamics and wall-related susceptibility in plant-pathogen interactions.*Frontiers in Plant Science,* 5, 228.

Bischoff, V., Cookson, S.J., Wu, S., Scheible, W.R. (2009) Thaxtomin A affects CESA-complex density, expression of cell wall genes, cell wall composition, and causes ectopic lignification in Arabidopsis thaliana seedlings. *Journal of Experimental Botany,* 60, 955–965.

Cano-Delgado, A., Penfield, S., Smith, C., Catley, M., Bevan, M. (2003) Reduced cellulose synthesis invokes lignification and defense responses in *Arabidopsis thaliana* . *The Plant Journal,* 34, 351-362.

Caplan, J.L., Mamillapalli, P., Burch-Smith, T.M., Czymmek, K. Dinesh-Kumar, S.P. (2008) Chloroplastic protein NRIP1 mediates innate immune receptor recognition of a viral effector. *Cell,* 132, 449–462.

Carriquí, M., Roig-Oliver, M., Brodribb, T.J., Coopman, R., Gill, W., Mark, K., Niinemets, Ü., Perera-Castro, A.V., Ribas-Carbó, M., Sack, L., Tosens, T., Waite, M., Flexas, J. (2019) Anatomical constraints to nonstomatal diffusion conductance and photosynthesis in lycophytes and bryophytes. *New Phytologist,* 222, 1256–1270.

Carriquí, M., Nadal, M., Clemente-Moreno, M.J., Gago, J., Miedes, E., Flexas, J. (2020) Cell wall composition strongly influences mesophyll conductance in gymnosperms. *The Plant Journal,* 103, 1372–1385.

Chen, Z., Yan, W., Sun, L., Tian, J., Liao, H. (2016) Proteomic analysis reveals growth inhibition of soybean roots by manganese toxicity is associated with alteration of cell wall structure and lignification.*Journal of Proteomics,* 143,151–160.

Chen, J., Zeng, B., Zhang, M., Xie, S., Wang, G., Hauck, A., Lai, J. (2014) Dynamic transcriptome landscape of maize embryo and endosperm development. *Plant Physiology,* 972, 252-264.

Cho, S., Purushotham, P., Fang, C., Maranas, C., Díaz-Moreno, S., Bulone, V., Zimmer, J., Kumar, M., Nixon, B.T. (2017) Synthesis and self-assembly of cellulose microfibrils from reconstituted cellulose synthase. *Plant Physiology,* 175, 146–156.

Court, D.L., Gan, J., Liang, Y.-H., Shaw, G.X., Tropea, J.E., Costantino, N., Waugh, D.S., Ji, X. (2013) RNase III: genetics and function; structure and mechanism. *Annual Review of Genetics,* 47, 405–431.

Dalisay, D.S., Kim, K.W., Lee, C., Yang, H., Rubel, O., Bowen, B.P., Davin, L.B., Lewis, N.G. (2015) Dirigent protein-mediated lignan and cyanogenic glucoside formation in flax seed: integrated omics and MALDI mass spectrometry imaging. *Journal of Natural Products,* 78, 1231–1242.

Davin, L.B., Lewis, N.G. (2000) Dirigent proteins and dirigent sites explain the mystery of specificity of radical precursor coupling in lignan and lignin biosynthesis. *Plant Physiology,* 123, 453–462.

Davin, L.B., Lewis, N.G. (2003) An historical perspective on lignan biosynthesis: monolignol, allylphenol and hydroxycinnamic acid coupling and downstream metabolism. *Phytochemistry Review,* 2, 257–288.

Denness, L., McKenna, J.F., Segonzac, C., Wormit, A., Madhou, P., Bennett, M., Mansfield, J., Zipfel, C., Hamann, T. (2011) Cell wall damage induced lignin biosynthesis is regulated by a reactive oxygen species- and jasmonic acid-dependent process in Arabidopsis. *Plant Physiology,* 156**,** 1364–1374.

Do, T.H.T., Martinoia, E., Lee, Y. (2018) Functions of ABC transporters in plant growth and development. *Current Opinion in Plant Biology,* 41, 32-38.

Effenberger, I., Zhang, B., Li, L., Wang, Q., Liu, Y., Klaiber, I., Pfannstiel, J., Wang, Q., Schaller, A. (2015) Dirigent proteins from cotton (*Gossypium* sp.) for the atropselective synthesis of gossypol. *Angewandte Chemie International Edition* , 54, 14660–14663.

Ellis, C., Karafyllidis, I., Wasternack, C., Turner, J.G. (2002) The*Arabidopsis* mutant *cev1* links cell wall signaling to jasmonate and ethylene responses. *Plant Cell,* 14, 1557–1566.

Ellsworth, P.V., Ellsworth, P.Z., Koteyeva, N.K., Cousins, A.B. (2018) Cell wall properties in Oryza sativa influence mesophyll CO_2 conductance. *New Phytologist,* 219, 66–76.

Engelsdorf, T., Gigli-Bisceglia, N., Veerabagu, M., McKenna, J.F., Vaahtera, L., Augstein, F., Van der Does, D., Zipfel, C., and Hamann, T. (2018) The plant cell wall integrity maintenance and immune signaling systems cooperate to control stress responses in Arabidopsis thaliana.*Science Signaling,* 11(536), eaao3070.

Engelsdorf, T., Kjaer L, Gigli-Bisceglia, N., Vaahtera, L., Bauer, S., Miedes, E., Wormit, A., James, L., Chairam, I., Molina, A., Hamann, T. (2019) Functional characterization of genes mediating cell wall metabolism and responses to plant cell wall integrity impairment.*BMC Plant Biology,* 19, 320-332.

Escudero, V., Jorda, L., Sopena-Torres, S., Mélida, H., Miedes, E., Muñoz-Barrios, A., Swami, S., Alexander, D., McKee, L.S., Sánchez-Vallet, A., et al. (2017) Alteration of cell wall xylan acetylation triggers defense responses that counterbalance the immune deficiencies of plants impaired in the β-subunit of the heterotrimeric G-protein. *The Plant Journal,* 92(3), 386-399.

Fernández-Calvino, L., Guzmán-Benito, I., Del Toro, F.J., Donaire, L., Castro-Sanz, A.B., Ruíz-Ferrer, V., and Llave, C. (2016) Activation of senescence-associated Dark-inducible (DIN) genes during infection contributes to enhanced susceptibility to plant viruses.*Molecular Plant Pathology,* 17(1), 3-15.

Fujiki, Y., Yoshikawa, Y., Sato, T., Inada, N., Ito, M., Nishida, I. and Watanabe, A. (2001) Dark-inducible genes from *Arabidopsis thaliana* are associated with leaf senescence and repressed by sugars.*Physiologia Plantarum,*111, 345–352.

Funatsuki, H., Suzuki, M., Hirose, A., Inaba, H., Yamada, T., Hajika, M., Komatsu, K., Katayama, T., Sayama, T., Ishimoto, M., et al. (2014) Molecular basis of a shattering resistance boosting global dissemination of soybean. *Proceedings of the National Academy of Sciences, USA,*111, 17797–17802.

Gasper, R., Effenberger, I., Kolesinski, P., Terlecka, B., Hofmann, E., and Schaller, A. (2016) Dirigent protein mode of action revealed by the crystal structure of AtDIR6. *Plant Physiology,* 172, 2165–2175.

Geldner, N. 2013. The endodermis. *Annual Review in Plant Biology,*64, 531–558.

Gigli-Bisceglia, N., Engelsdorf, T., and Hamann, T. (2020) Plant cell wall integrity maintenance in model plants and crop species-relevant cell wall components and underlying guiding principles. *Cellular and Molecular* Life *Sciences,* 77(11), 2049-2077.

He, X., Zhu, L., Wassan, G.M., Wang, Y., Miao, Y., Shaban, M., Hu, H., Sun, H., Zhang, X. (2018) GhJAZ2 attenuates cotton resistance to biotic stresses via the inhibition of the transcriptional activity of GhbHLH171. *Molecular Plant Pathology,* 19(4), 896-908.

Hernandez-Blanco, C., Feng, D.X., Hu, J. Sánchez-Vallet, A., Deslandes, L., Llorente, F., Berrocal-Lobo, M., Keller, H., Barlet, X., Sánchez-Rodríguez, C., et al. (2007) Impairment of cellulose synthases required for Arabidopsis secondary cell wall formation enhances disease resistance. *Plant Cell,* 19, 890–903.

Hosmani, P.S., Kamiya, T., Danku, J., Naseer, S., Geldner, N., Guerinot, M.L., Salt, D.E. (2013) Dirigent domain-containing protein is part of the machinery required for formation of the lignin-based Casparian strip in the root. *Proceedings of the National Academy of Sciences, USA,* 110, 14498–14503.

Houston, K., Tucker, M.R., Chowdhury, J., Shirley, N. Little, A. (2016) The plant cell wall: a complex and dynamic structure as revealed by the responses of genes under stress conditions. *Frontiers in Plant Science,* 7, 984.

Huot, B., Yao, J., Montgomery, B.L., He, S. Y. (2014) Growth-defense tradeoffs in plants: a balancing act to optimize fitness.*Molecular Plant,* 7, 1267-1287.

Jiao S, Hazebroek JP, Chamberlin MA, Perkins M, Sandhu AS, Gupta R, Simcox KD, Yinghong L, Prall A, Heetland L, et al. (2019) Chitinase-like1 Plays a Role in Stalk Tensile Strength in Maize. *Plant Physiology,* 181(3), 1127-1147.

Kesten, C., Menna, A. Sanchez-Rodrıguez, C. (2017) Regulation of cellulose synthesis in response to stress. *Current Opinion in Plant Biology,* 40, 106–113.

Kotake, T., Aohara, T., Hirano, K., Sato, A., Kaneko, Y., Tsumuraya, Y., Takatsuji, H., Kawasaki, S. (2011) Rice *brittle culm 6* encodes a dominant-negative form of CesA protein that perturbs cellulose synthesis in secondary cell walls.*Journal of Experimental Botany,* 62, 2053–2062.

Lampugnani, E.R., Khan, G.A., Somssich, M., Persson, S. (2018) Building a plant cell wall at a glance. *Journal of Cell Science,* 131(2), jcs207373.

Li, F., Xie, G., Huang, J., Zhang, R., Li, Y., Zhang, M., Wang, Y., Li, A., Li, X., Xia, T., et al. (2017) OsCESA9 conserved-site mutation leads to largely enhanced plant lodging resistance and biomass enzymatic saccharification by reducing cellulose DP and crystallinity in rice. *Plant Biotechnology Journal,* 15, 1093–1104.

Li, F., Zhang, M., Guo, K., Hu, Z., Zhang, R., Feng, Y., Yi, X., Zou, W., Wang, L., Wu, C., et al. (2015) High-level hemicellulosic arabinose predominately affects lignocellulose crystallinity for genetically enhancing both plant lodging resistance and biomass enzymatic digestibility in rice mutants. *Plant Biotechnology Journal,* 13(4), 514–525.

Li, N., Lin, B., Wang, H., Li, X., Yang, F., Ding, X., Yan, J., and Chu, Z. (2019) Natural variation in ZmFBL41 confers banded leaf and sheath blight resistance in maize. *Nature Genetics,* 51(10), 1540-1548.

Liu, Q., Luo, L., and Zheng, L. (2018) Lignins: biosynthesis and biological functions in plants. *International Journal of Molecular Science,* 19, 335–341.

Lu, X.D., Liu, J.S., Ren, W., Yang, Q., Chai, Z.G., Chen, R.M., Wang. L., et al. (2018) Gene-indexed mutations in maize. *Molecular Plant,* 11, 496–504.

Lu, Y., Yao, J. (2018) Chloroplasts at the Crossroad of Photosynthesis, Pathogen Infection and Plant Defense.

International Journal of Molecular Science, 19(12), 3900.

Miedes, E., Vanholme, R., Boerjan, W., Molina, A. (2014) The role of the secondary cell wall in plant resistance to pathogens. *Frontiers in Plant Science,* 5, 358–368.

Ohtani, M., Demura, T. (2019) The quest for transcriptional hubs of lignin biosynthesis: beyond the NAC-MYB-gene regulatory network model. *Current Opinion in Biotechnology,* 56, 82–87.

Onoda, Y., Wright, I.J., Evans, J.R., Hikosaka, K., Kitajima, K., Niinemets, Ü., Poorter, H., Tosens, T., Westoby, M. (2017) Physiological and structural tradeoffs underlying the leaf economics spectrum. *New Phytologist,* 214, 1447–1463.

Paniagua, C., Bilkova, A., Jackson, P., Dabravolski, S., Riber, W., Didi, V., Houser, J., Gigli-Bisceglia, N., Wimmerova, M., Budínská, E., et al. (2017) Dirigent proteins in plants: modulating cell wall metabolism during abiotic and biotic stress exposure. *Journal of Experimental Botany,* 68(13), 3287-3301.

Pickel, B., Constantin, M.A., Pfannstiel, J., Conrad, J., Beifuss, U., Schaller, A. (2010) An enantiocomplementary dirigent protein for the enantioselective laccase-catalyzed oxidative coupling of phenols. Angew*andte Chemie International edtion,* 49, 202–204.

Pogorelko, G., Lionetti, V., Bellincampi, D., Zabotina, O. (2013) Cell wall integrity: targeted post-synthetic modifications to reveal its role in plant growth and defense against pathogens. *Plant Signaling &Behavior,* 8(9), e25435.

Ralph, J., Lapierre, C., Boerjan, W. (2019) Lignin structure and its engineering. *Current Opinion in Biotechnology,* 56, 240–249.

Rehman, H., Nawaz, M., Shah, Z., Ludwig-Müller, J., Chung, G., Ahmad, M., Yang, S., Lee, S. (2018) Comparative genomic and transcriptomic analyses of Family-1 UDP glycosyltransferase in three Brassica species and Arabidopsis indicates stress responsive regulation. *Scientific Reports,* 8(1), 1875.

Roig-Oliver, M., Rayon, C., Roulard, R., Fournet, F., Bota, J., Flexas, J. (2021) Reduced photosynthesis in Arabidopsis thaliana *atpme17.2* and *atpae11.1* mutants is associated to altered cell wall composition. *Physiologia Plantarum,* 172(3), 1439-1451.

Roppolo, D., De Rybel, B., Dénervaud, T.V., Pfister, A., Alassimone, J., Vermeer, J.E., Yamazaki, M., Stierhof, Y.D., Beeckman, T., and Geldner, N. (2011) A novel protein family mediates Casparian strip formation in the endodermis. *Nature,* 473, 380–383.

Rui, Y., Dinneny, J.R. (2020) A wall with integrity: surveillance and maintenance of the plant cell wall under stress.*New Phytologist,* 225(4), 1428-1439.

Schneider, R., Tang, L., Lampugnani, E.R., Barkwill, S., Lathe, R., Zhang, Y., McFarlane, H.E., Pesquet, E., Niittyla, T., Mansfield, S.D., et al. (2017) Two complementary mechanisms underpin cell wall patterning during xylem vessel development. *Plant Cell,* 29, 2433–2449.

Seneviratne, H.K., Dalisay, D.S., Kim, K.W., Moinuddin, S.G., Yang, H., Hartshorn, C.M., Davin, L.B., Lewis, N.G. (2015) Non-host disease resistance response in pea (Pisum sativum) pods: biochemical function of DRR206 and phytoalexin pathway localization. *Phytochemistry,* 113, 140–148.

Tanaka, K., Murata, K., Yamazaki, M., Onosato, K., Miyao, A., Hirochika, H. (2003) Three distinct rice cellulose synthase catalytic subunit genes required for cellulose synthesis in the secondary wall. *Plant Physiology,* 133, 73–83.

Taylor-Teeples, M., Lin, L., De Lucas, M., Turco, G., Toal, T.W., Gaudinier, A., Young, N.F., Trabucco, G.M., Veling, M.T., Lamothe, R., et al. (2015) An Arabidopsis gene regulatory network for secondary cell wall synthesis. *Nature,* 517, 571–575.

Tsang, D.L., Edmond, C., Harrington, J.L., Nuhse, T.S. (2011) Cell wall integrity controls root elongation via a general 1-aminocyclopropane-1-carboxylic acid-dependent, ethylene-independent pathway. *Plant Physiology,* 156, 596–604.

Vaahtera, L., Schulz, J., Hamann, T. (2019) Cell wall integrity maintenance during plant development and interaction with the environment.*Nature Plants,* 5(9), 924-932.

Veromann-Jürgenson, L., Tosens, T., Laanisto, L., Niinemets, Ü. (2017) Extremely thick cell walls and low mesophyll conductance: welcome to the world of ancient living! *Journal of Experimental Botany,* 68, 1639–1653.

Wang, D., Qin, Y., Fang, J., Yuan, S., Peng, L., Zhao, J., Li, X. (2016) A missense mutation in the zinc finger domain of OsCESA7 deleteriously affects cellulose biosynthesis and plant growth in Rice. *PLoS One* , 11, e0153993.

Wang G, Sun X, Wang G, Wang F, Gao Q, Sun X, Tang Y, Chang C, Lai J, Zhu L, et al. (2011) *Opaque7* encodes an acyl-activating enzymelike protein that affects storage protein synthesis in maize endosperm.*Genetics,* 189, 1281–1295.

Yang, N., Lu, Y., Yang, X., Huang, J., Zhou, Y., Ali, F., Wen, W., Liu, J., Li, J., Yan, J. **(** 2014) Genome wide association studies using a new nonparametric model reveal the genetic architecture of 17 agronomic traits in an enlarged maize association panel. *PLoS Genetics* **, 10** , e1004573.

Yang, Q., Yin, G. M., Guo, Y. L., Zhang, D. F., Chen, S. J., Xu, M. L. (2010) A major QTL for resistance to Gibberella stalk rot in maize.*Theoretical and Applied Genetics,* 121, 673–687.

Yang, S., Berberich, T., Miyazaki, A., Sano, H., Kusano, T. (2003)*Ntdin* , a tobacco senescence-associated gene, is involved in molybdenum cofactor biosynthesis. *Plant Cell Physiology,* 44(10), 1037–1044.

Ye, J., Guo, Y., Zhang, D., Zhang, N., Wang, C., Xu, M. (2013) Cytological and molecular characterization of QTL-qRfg1 which confers resistance to *gibberella* stalk-rot disease in maize.*Molecular Plant–Microbe Interactions,* 26, 1417–1428.

Ye, J., Zhong, T., Zhang, D., Ma, C., Wang, L., Yao, L., Zhang, Q., Zhu, M., Xu, M. (2018) The maize auxin-regulated protein ZmAuxRP1 coordinates the balance between growth and defense. *Molecular Plant,* 12, 360–373.

Yonekura-Sakakibara, K., Yamamura, M., Matsuda, F., Ono, E., Nakabayashi, R., Sugawara, S., Mori, T., Tobimatsu, Y., Umezawa, T., Saito, K. (2021) Seed-coat protective neolignans are produced by the dirigent protein AtDP1 and the laccase AtLAC5 in Arabidopsis. *Plant Cell,* 33(1), 129-152.

Zhan, J., Thakare, D., Ma, C., Lloyd, A., Nixon, N.M., Arakaki, A.M., Burnett, W.J., Logan, K.O., Wang, D., Wang, X., et al. (2015) RNA sequencing of laser-capture microdissected compartments of the maize kernel identifies regulatory modules associated with endosperm cell differentiation. *Plant Cell,* 27, 513–531.

Zhang, Q., Zhong, T., E, *L.* , Xu, M., Dai, W., Sun, S. Ye, J. (2021) GT Factor ZmGT-3b Is Associated With Regulation of Photosynthesis and Defense Response to *Fusarium graminearum* Infection in Maize Seedling. *Frontiers in Plant Science,* 12, 724133.

Zhang, R., Hu, H., Wang, Y., Hu, Z., Ren, S., Li, J., He, B., Wang, Y., Xia, T., Chen, P., et al. (2020) A novel rice *fragile culm 24* mutant encodes a UDP-glucose epimerase that affects cell wall property and photosynthesis. *Journal of Experimental Botany,* 71, 2956–2969.

Figure Legends

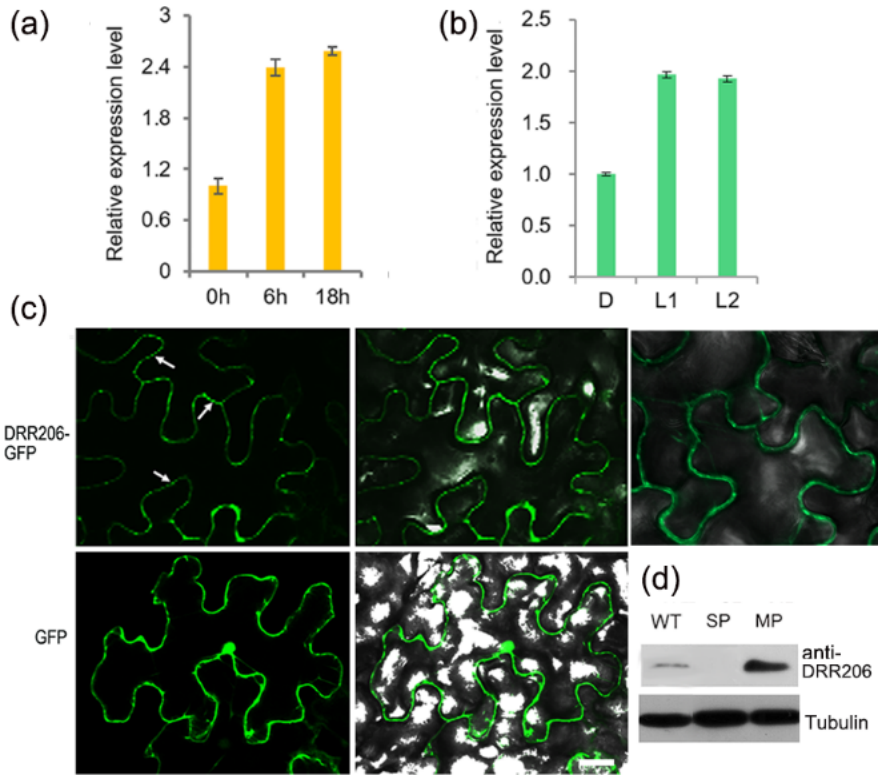

FIGURE 1 The light and pathogen inducible expression of *ZmDRR206* and the plasma-membrane localization of ZmDRR206. (a) The fungus-inducible expression of *ZmDRR206* . 0h, 6h and 18h are the WT seedlings at 0h, 6h and 18h after inoculation with *F. graminearum* , respectively. (b) The light-inducible expression of *ZmDRR206* . D is the WT seedlings grew under continuous dark for 5 days after germination (DAG), L1 and L2 are the dark-grown 5-DAG WT seedlings transferred to light for 1 h and 2 h, respectively. (c) The ZmDRR206-GFP fluorescence signal is predominantly associated with the periphery of the leaf cells detected by confocal microscopy. The arrows indicate the punctate ZmDRR206-GFP signal distribution in the cell periphery. Bar=20μm. (d) ZmDRR206 protein is detected in the membrane pellet (MP) with ZmDRR206-specific antibody by western-blot analysis. The total protein (WT), the soluble protein (SP) and MP were extracted from 6-DAG WT seedlings.

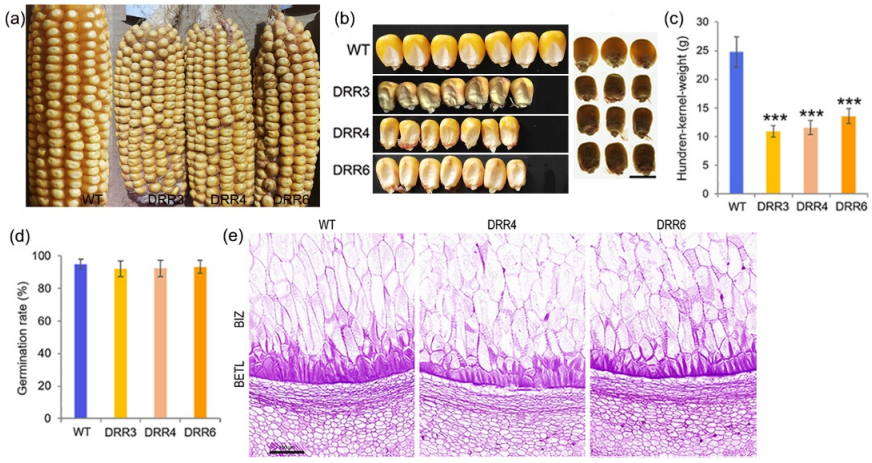

FIGURE 2 The mature kernel characterizations of transgenic maize lines overexpressing *Zm-DRR206*. **(** a) The ear phenotypes of the wild-type (WT) and *ZmDRR206* over-expressing (*DRR-OE*) lines. (b) The mature kernel phenotypes of the WT and *DRR-OE*lines. *DRR-OE* kernels were small, opaque and shriveled at the bottom. (c) The hundred kernel weight of the WT and *DRR-OE* lines. (d) The kernel germination rate of the WT and *DRR-OE* lines. Data are presented as mean values ± SD of three replicates per genotype are presented. The asterisks represent a significant difference at $^{**}P < 0.01$, $^{***}p < 0.001$, according to a paired Student's t -test. (e) The wall-in-growth in the basal endosperm transfer layer (BETL) and the cell phenotype in the basal intermediate zone (BIZ) in developing maize kernels. Bar=100 μm. WT is the wild type inbred line LH244, *DRR3* , *DRR4* and*DRR6* are *ZmDRR206* over-expressing transgenic everts*DRR-OE3* , *DRR-OE4* and*DRR-OE6* .

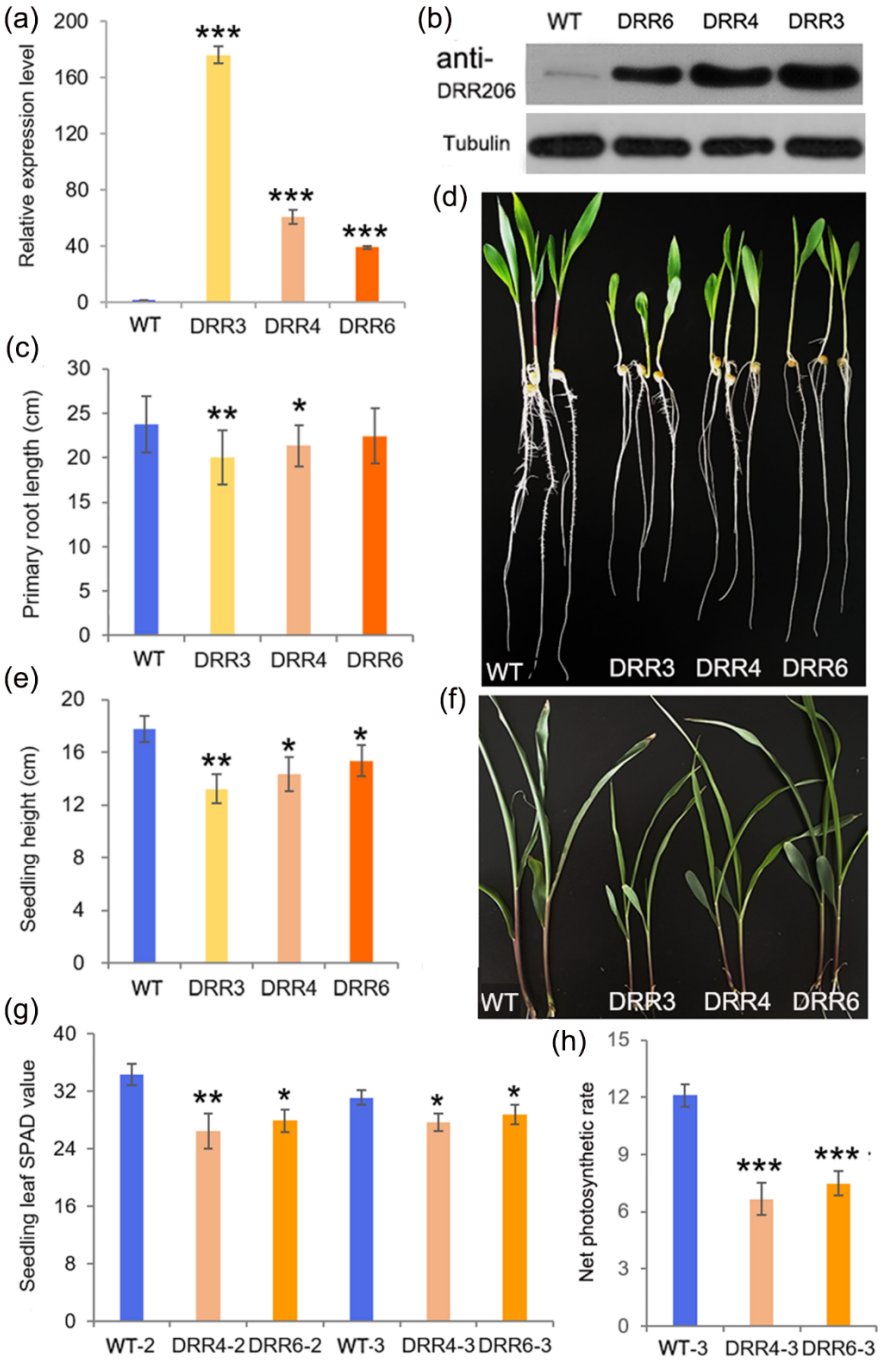

FIGURE 3 Seedling growth phenotypes of transgenic maize lines overexpressing *ZmDRR206*. (a-b) The transcript (a) and protein (b) levels of *ZmDRR206* in the WT and *DRR-OE* seedlings. ZmDRR206 specific antibody was used to for the western-blot analysis with total proteins extracted from maize young seedlings at 6-DAG. (c-d) The primary root length (c) and the seedling phenotypes (d) of the WT and *DRR-OE* lines. Data are presented as mean values ± SD, n > 10 independent seedlings. (e-f) The seedling height (e) and phenotypes (f) of the WT and *DRR-OE* lines at 12-DAG. Data are presented as mean values ± SD, n > 10 independent seedlings. (g) The SPAD value of the WT and *DRR-OE* lines at 12- or 15-DAG.

Data are presented as mean values ± SD, n > 10 independent seedlings. (h) The net photosynthetic rate of the WT and*DRR-OE* lines at 15-DAG. Data are presented as mean values ± SD, n = 5 independent seedlings. -2 and -3 were the 2nd and the 3rd expanded leaf used for SPAD value and Pn analysis from the 12-DAG seedlings and 5-DAG seedlings, respectively. WT is the wild type line LH244, *DRR3* , *DRR4* and *DRR6*are *ZmDRR206* over-expressing transgenic everts *DRR-OE3* ,*DRR-OE4* and *DRR-OE6* . The asterisks represent a significant difference at *p <0.05, ** P < 0.01, ***p <0.001, according to a paired Student'st -test.

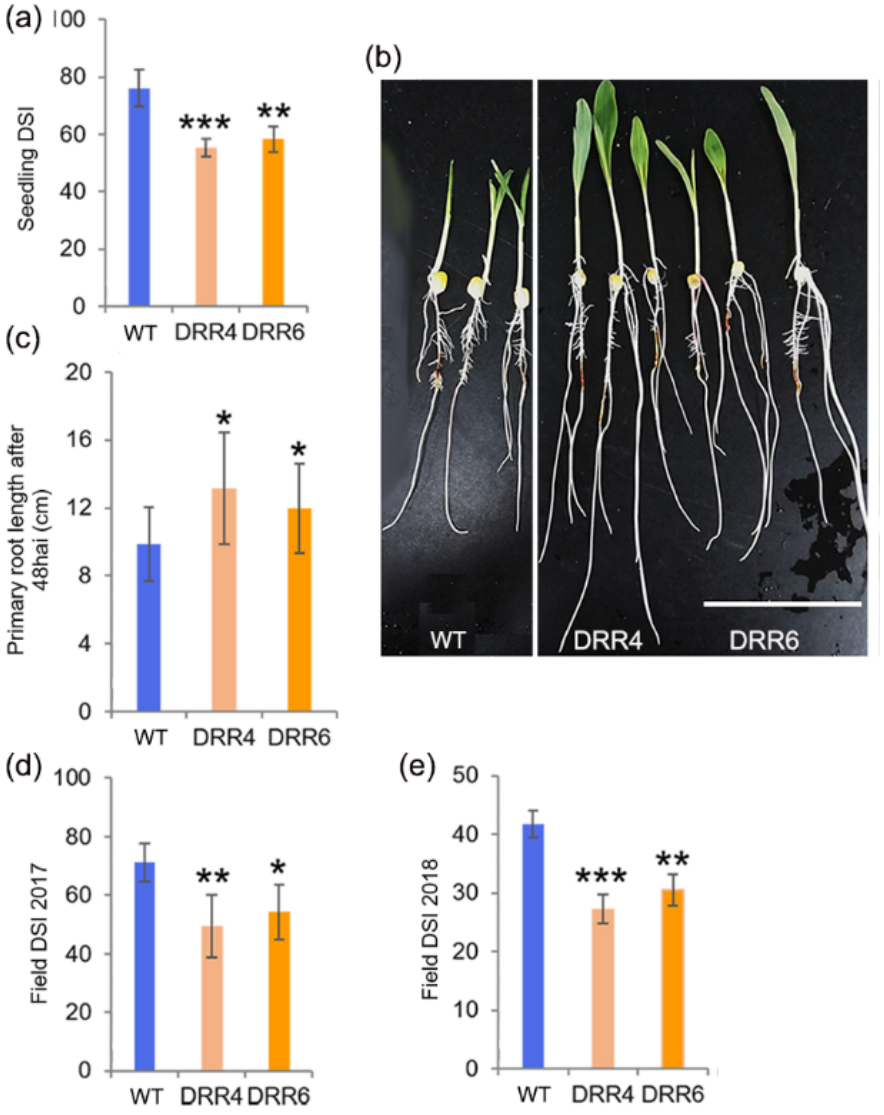

FIGURE 4 Disease resistance phenotypes of transgenic maize lines overexpressing *ZmDRR206*. (a) The DSI of the WT and *DRR-OE*seedlings after *F. graminearum* inoculation. Data are presented as mean values ± SD, n > 15 independent seedlings. (b-c) The growth phenotype (b) and the primary root length (c) of the inoculated WT and *DRR-OE* seedlings with severe disease symptom. Data are presented as mean values ± SD, n > 15 independent seedlings. (d-e) The DSI of the inoculated WT and *DRR-OE* mature plants after *F. graminearum* inoculation in the field in 2017 (d) and 2018 (e). Data are presented as mean values ± SD, n > 30 independent plants. WT is the wild type line LH244, *DRR4* and*DRR6* are *ZmDRR206*

over-expressing transgenic everts*DRR-OE4* and *DRR-OE6* . The asterisks represent a significant difference at * p <0.05, ** P< 0.01, *** p <0.001, according to a paired Student's t -test.

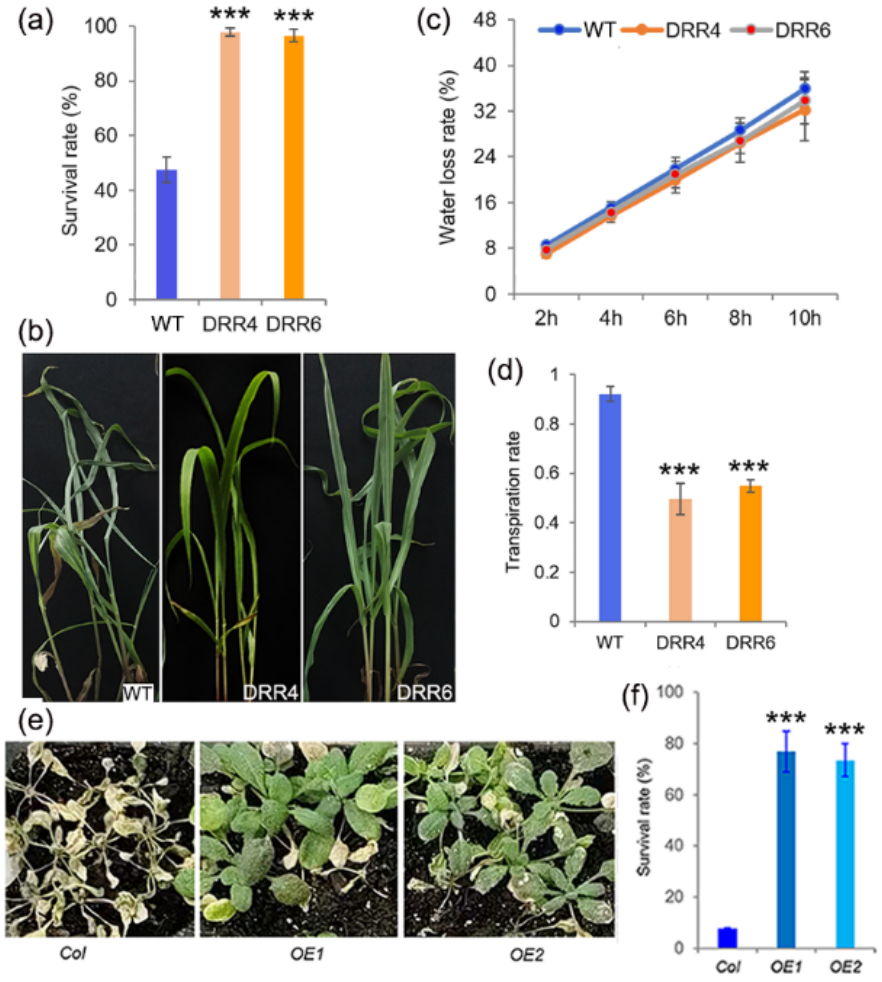

FIGURE 5 Drought tolerance phenotypes of transgenic plants overexpressing *ZmDRR206*. (a-b) The survival rate (a) and the growth phenotype (b) of the WT and *DRR-OE* seedlings after drought treatment. Data are presented as mean values ± SD, n > 15 seedlings with three independent biological repeats. (c) The water loss rate of the latest expanded leaf of the15-DAG WT and *DRR-OE*seedlings. Data are presented as mean values ± SD, n = 5 seedlings with three independent biological repeats. (d) The transpiration rate of the latest expanded leaf of the 15-DAG WT and *DRR-OE* seedlings. -3 were the 3rd expanded leaf used for transpiration rate analysis. Data are presented as mean values ± SD, n = 5 seedlings. WT is the wild type line LH244, *DRR4* and *DRR6* are*ZmDRR206* over-expressing transgenic everts *DRR-OE4* and*DRR-OE6* . (e-f) The growth phenotype (e) and the survival rate (f) of the Col and *DRR-OE* transgenic Arabidopsis seedlings after drought treatment. Col is the wild-type and *OE1* , *OE2* are two independent *ZmDRR206* overexpression transgenic Arabidopsis lines. Data are presented as mean values ± SD, n > 25 seedlings with three independent biological repeats. The asterisks represent a significant difference at *** p <0.001, according to a paired Student's t -test.

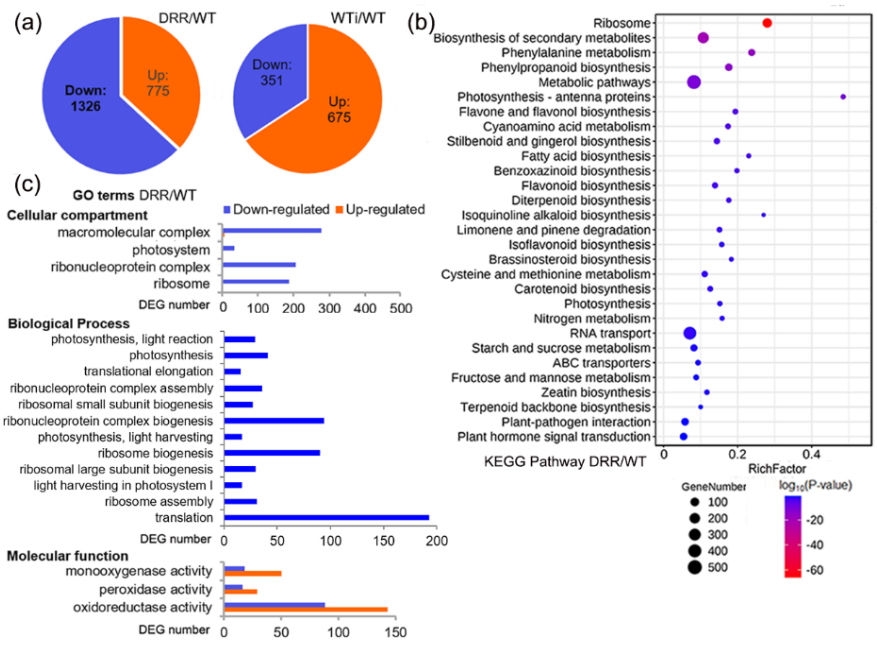

FIGURE 6 Changes in the transcriptome induced by *ZmDRR206* overexpression in maize seedling. (a) The numbers of differentially expressed genes (DEGs) induced by *ZmDRR206* overexpression or inoculation. Compared to WT, *ZmDRR206* overexpression induced 2101 DEGs (DRR/WT), while *F. graminearum* inoculation induced 1,026 DEGs (WTi/WT). DRR represents *DRR-OE* seedlings grown under normal conditions without inoculation, WT and WTi represent wild-type seedlings without and with inoculation, respectively. (b) The top-enriched KEGG pathway of the DEGs from DRR/WT transcriptome pair. Circle sizes indicate DEG numbers and the color gradients indicate enrichment significance. (c) The significant enrichment of ZmDRR206 down-regulated genes in translation- and photosynthesis-related functional categories and the enzyme activity of the up-regulate genes.

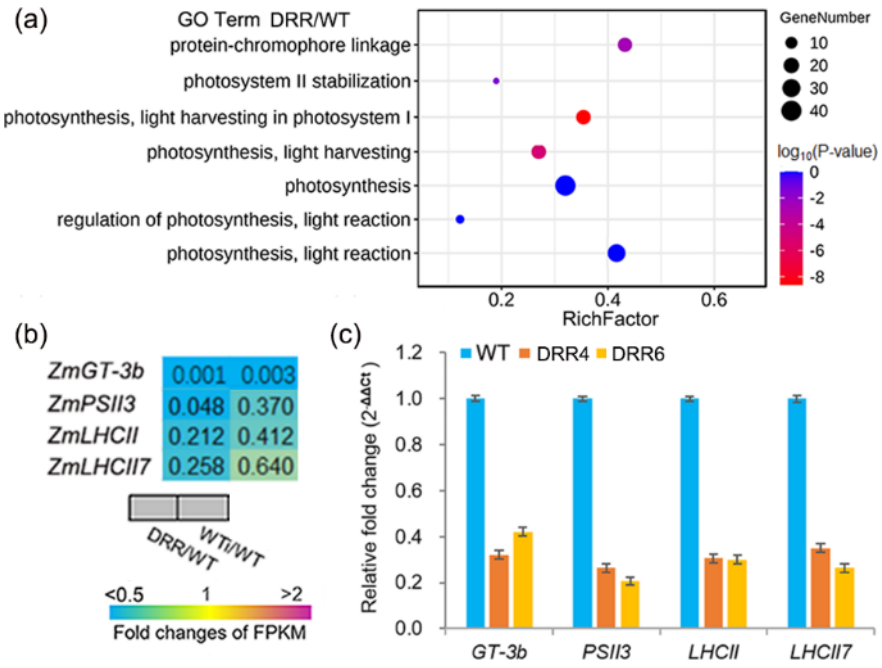

FIGURE 7 The constitutive down-regulation of photosynthesis-related genes in transgenic maize seedlings overexpressing *ZmDRR206*. (a) The significant enrichment of the ZmDRR206 down-regulated genes in photosynthesis-related functional categories. Circle sizes indicate DEG numbers and the color gradients indicate enrichment significance. (b-c) The expression of photosynthesis-related genes was down-regulated in*DRR206 -OE* seedlings, by transcriptome sequencing (b) and by RT-qPCR (c). *Zm-DRR206* overexpression (DRR) and WT (LH244) maize seedlings at 6-DAG with (WTi) or without inoculation (WT, DRR). The numerical values are the ratios (DRR/WT or WTi/WT) of the DGEs, and the background color showed the gene relative expression levels (red represents up-regulated, blue is down-regulated, and yellow is no significant change). Values presented in (c) are the means ± SD of three replicates per genotype. WT is the wild type line LH244, *DRR4* and*DRR6* are two *ZmDRR206* over-expressing transgenic everts*DRR-OE4* and *DRR-OE6* .

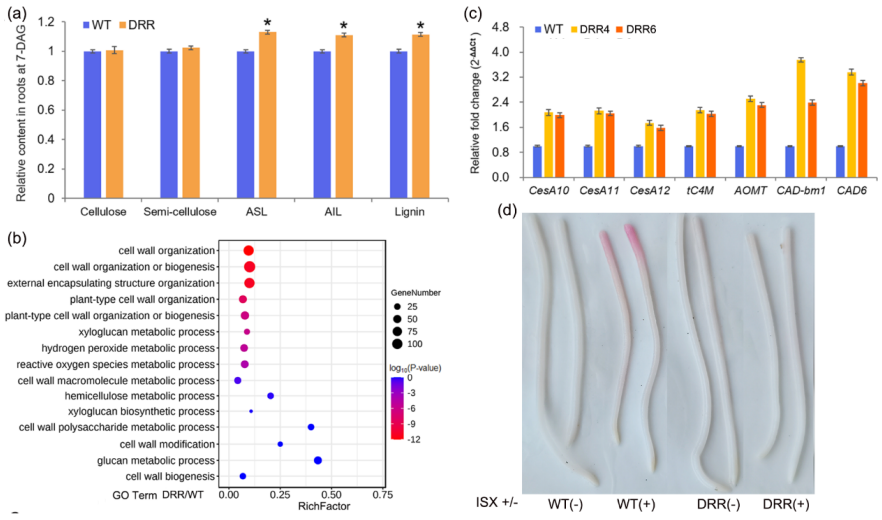

FIGURE 8 The role of *ZmDRR206* in cell wall integrity maintenance during maize seedling growth. (a) The contents of major cell wall components in 7-DAG maize seedling roots. ASL, acid soluble lignin, AIL, acid insoluble lignin. Values presented are the means ± SD of three replicates per genotype. The asterisks represent a significant difference at $*p < 0.05$, according to a paired Student's t -test. (b) The significant enrichment of the DEGs induced by *ZmDRR206*- overexpression in cell wall organization/ biogenesis related functional categories. Circle sizes indicate DEG numbers and the color gradients indicate enrichment significance. (c) The constitutive upregulation of the cell wall biosynthesis related genes in 6-DAG *DRR-OE* seedlings by RT-qPCR.*tC4M* , Trans-cinnamate 4-monooxygenase, *AOMT* , Caffeoyl-CoA O-methyltransferase1, *CAD-bm1* /*CAD6* , cinnamyl alcohol dehydrogenases. WT represent LH244 seedlings, *DRR4* and*DRR6* are *ZmDRR206* over-expressing transgenic everts*DRR-OE4* and *DRR-OE6* . Values are the means ± SD of three replicates per genotype are presented. (d) *DRR-OE* seedlings are resistant to isoxaben (ISX, a cellulose biosynthesis inhibitor). The apical part of ISX-treated WT primary root tips was stained red, while the ISX-treated *DRR-OE* seedling root wasn't, by a lignin-specific phloroglucinol-HCl staining.

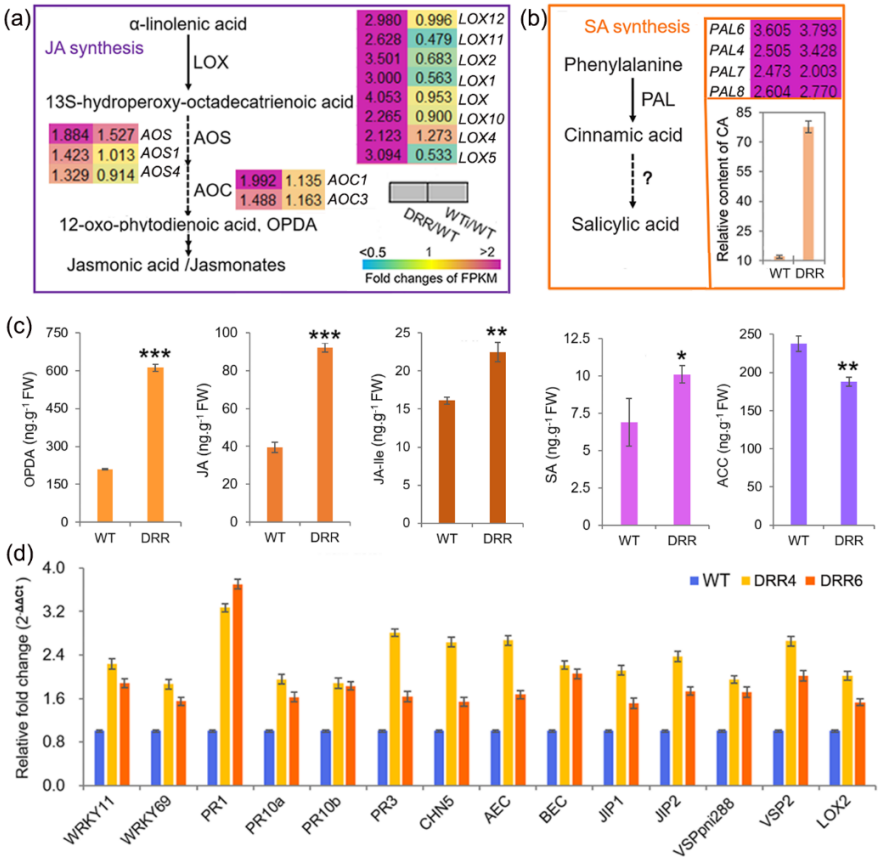

FIGURE 9 The altered biosynthesis of phytohormones and the constitutive expression of defense-related genes in *DRR-OE* seedling. (a) The constitutive upregulation of the JA biosynthesis-related genes in *DRR-OE*seedlings. LOX is lipoxygenase, AOS is allene oxide synthase, AOC is allene oxide cyclase. (b) The *PAL* genes and the precursor for SA biosynthesis were constitutively upregulated in *DRR-OE* seedling. PAL is phenylalanine ammonia-lyase. CA is cinnamic acid. The data was from transcriptome sequencing of *DRR-OE* and WT (LH244) seedlings at 6-DAG with (WTi) or without inoculation (WT, DRR). The numerical values are the ratios (DRR/WT, WTi/WT) of the DGEs, the background color showed the gene relative expression levels in the transcriptome pair (red represents up-regulated, blue is

down-regulated, and yellow is no significant change). (c) The contents of the phytohormones in WT and *DRR-OE* seedlings at 6-DAG. JA-Ile (Jasmonoyl-isoleucine) is the active form of JA; OPDA (12-oxo-phytodienoic acid) is the precursor for JA biosynthesis; ACC (1-Aminocyclopropane-1-carboxylate) is the precursor for ethylene biosynthesis. Values are the means ± SD of three replicates per genotype are presented. The asterisks represent a significant difference at * p <0.05, ** P< 0.01, *** p <0.001, according to a paired Student's t -test. (d) The constitutive upregulation of the defense-related genes in *DRR-OE* seedling by RT-qPCR. WRKY TF encoding genes (*WRKY11* , *WRKY69*), PR genes (*PR1* ,*PR10a* , *PR10b* and *PR3*), chitinase genes (*CHN5* , *AEC* and *BEC*), the JA regulated genes (two*JIP* s, two *VSP* s, and *LOX2*). WT represents LH244 seedlings, *DRR4* and *DRR6* are *ZmDRR206*over-expressing transgenic everts *DRR-OE4* and *DRR-OE6* . Values are the means ± SD of three replicates per genotype are presented.

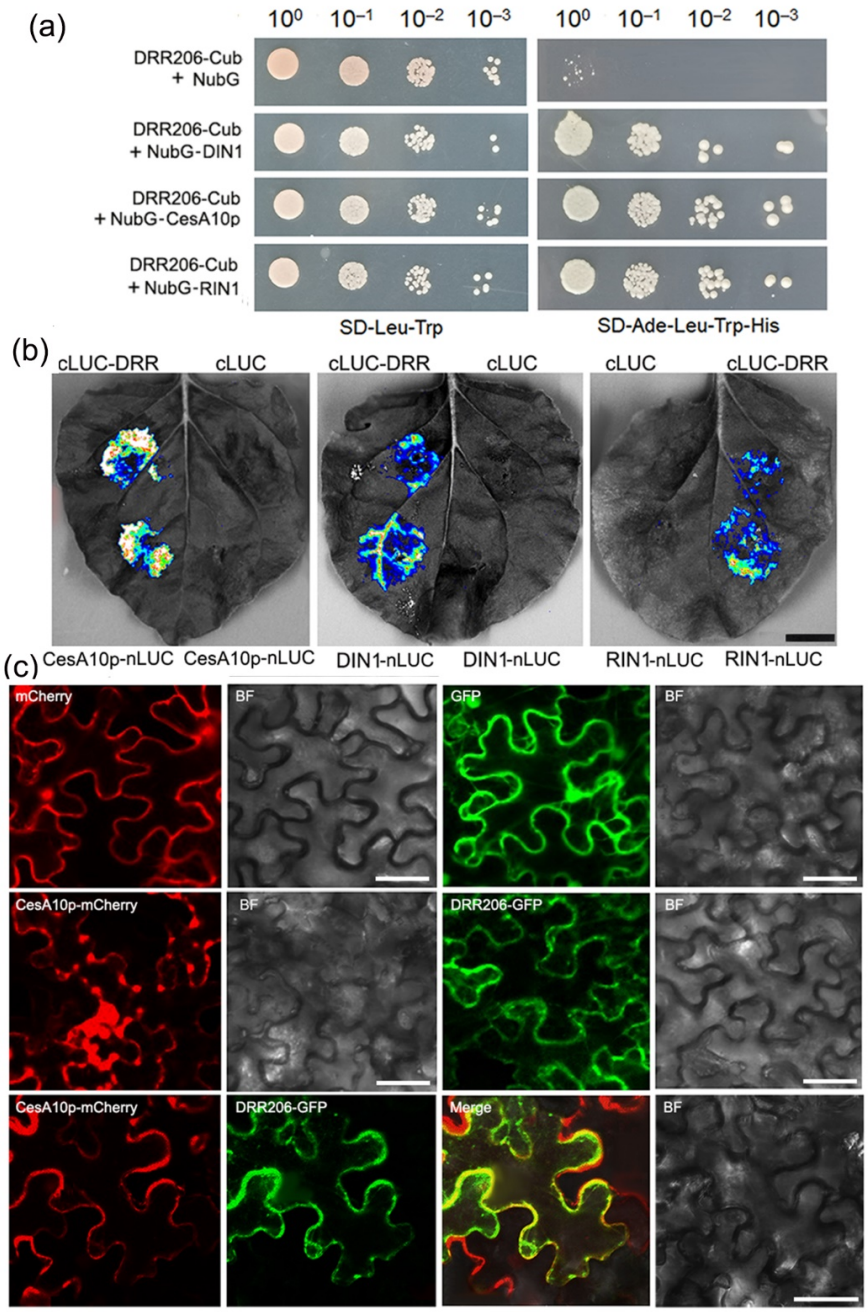

FIGURE 10 The physical interaction between ZmDRR206 and its protein partners in yeast and in *planta* . (a) Y2H assays between ZmDRR206 and ZmCesA10, ZmDRR206 and ZmDIN1, ZmDRR206 and ZmRIN1. The NMY51 yeast cells co-transformed with *DRR206-Cub* and*NubG-CesA10p* or *DRR206-Cub* and *NubG-DIN1* , or*DRR206-Cub* and *NubG-RIN1* constructs, grew well on synthetic dropout (SD) medium without Ade, Leu, Trp, His (right panel, SD/-Ade-Leu-Trp-His) selective medium, but not the control combination*DRR206-Cub* and NubG vector. (b) The interaction between ZmDRR206 and ZmCesA10, ZmDRR206 and ZmDIN1, ZmDRR206 and ZmRIN1 by LCI assay in*N. benthamiana* . The overlapping signal of luciferase and light was shown. cLUC, C-terminal LUC; nLUC, N-terminal LUC. The fluorescent signal

intensity represents their interaction activities. The combinations used for interaction between ZmDRR206 and the protein of interest are labeled, the combination between cLUC and the protein of interest show the signals of the negative controls. These experiments were conducted three times with similar results. Scale bar, 1 cm. (c) DRR206-GFP could co-localize with CesA10p-mCherry in the periphery of leaf cells. Both DRR206-GFP and CesA10p-mCherry fluorescence signal predominantly localized in cell periphery of the intact leaf tissue, and CesA10p-mCherry accumulated into big spots in cell periphery. The*N. benthamiana* leaves were infiltrated with agrobacterium that contained *pSuper* : *mCherry* , or *pCaMV35S* : *GFP*or *pCaMV35S* : *ZmDRR206-GFP* and/or *pSuper* :*ZmCesA10p-mCherry* . Bar=20μm.

Hosted file

`Suppl table S 0620.xlsx` available at https://authorea.com/users/498498/articles/579261-zmdrr206-involves-in-maintaining-cell-wall-integrity-during-maize-seedling-growth-and-interaction-with-the-environment